공학석사 학위논문

극지용 DP보조계류시스템을 위한 새로운 위치유지 전략개발

Development of new station-keeping strategy for DP assisted mooring system in Arctic Ocean

지도교수 이 승 재

2019 년 2 월

한국해양대학교 대학원

조선해양시스템공학과

최 솔 미

본 논문을 최솔미의 공학석사 학위논문으로 인준함.

위원장 이 성 욱 (인)

위 원 이 승 재 (인)

위 원 이 재 용 (인)

2018년 12월 07일

한국해양대학교 대학원

Contents

List of Tables

List of Figures

List of Figures

Development of new station-keeping strategy for DP assisted mooring system in Arctic Ocean

Choi, Sol Mi

Department of Naval Architecture and Ocean Systems Engineering
Graduate School of Korea Maritime and Ocean University

초 록

극지방용 부유식 해양구조물의 위치유지시스템은 일반적인 환경과 다르게 유빙의 특성을 고려한 위치유지 전략이 필요하다. DP 보조계류시스템은 위치유지를 위해 가장 널리 사용되는 계류와 DP 시스템이 결합된 형태로 이러한 극한의 환경에 적합한 솔루션으로 주목받고 있다. 하지만, 쇄빙이 선행되어도 구조물 주변에 축적되는 빙 특성으로 인해 구조물의 과도한 표류가 발생할 수 있고 계류시스템의 파단 위험이 상승할 수 있다. 따라서, 극지용 DP 시스템은 해역의 빙 특성을 고려하여 구조물의 안전을 보장할 수 있는 제어 전략을 수립해야한다. 본 논문에서는 구조물에 유발되는 빙의 부하를 최소화하고 안정적인 운용을 가능하게 하는 DP 보조계류시스템의 새로운 제어 전략을 제시하고자 한다. 새로운 제어전략은 계류선 장력을 이용한 구조물의 위치제어와 빙 표류방향에 대한 방향제어로 구성하였다. 선행적으로 구조물의 위치와 계류선 장력을 지속적으로 안전범위에 유지시킬 수 있는 DP 보조계류시스템용 위치제어인 Set point (SP)제어법을 제시하였다. 그 후, 다양한 빙 조건에서 DP 시스템의 정적해석을 수행하여 대빙 위치유지성능의 특성을 파악하였다.

본 결과를 토대로 빙의 부하를 최소화하기 위한 방향제어를 개발하였으며 최종적으로 극지방용 DP 보조계류시스템의 제어전략을 수립하였다.

Abstract

The control strategy for a station keeping of floating offshore platform in Arctic ocean should consider characteristics of ice load unlike normal sea. The Dynamic Positioning (DP) assisted mooring system which is a combination of mooring and DP system has been noted as an appropriate solution for severe environmental condition like Arctic ocean. However, even if the breaking of ice is preceded, accumulation of ice floes around platforms can increase the risks such as the excessive drift and failure of mooring system. As a result, DP system in this condition should establish a proper control strategy which can ensure the safety of platform considering the characteristics of ice load.

In this paper, a new station keeping strategy to minimize the load of platform caused by ice loads and enable safety operation is suggested. The new strategy is consisted of the position control using mooring tension and heading control considering the direction of ice drift. Firstly, Position control named Set point(SP) control is suggested which can keep the position and mooring tension in permissible range. Subsequently, DP capability analysis in various ice condition is conducted to investigate characteristics of station keeping quality against ice loads. Using the result of DP capability analysis, the heading control to minimize the load from ice is developed. As a result, a new control strategy for DP assisted mooring system under ice condition is established.

KEY WORDS: Dynmaic Positioning System 동적위치유지시스템; DP assisted mooring system DP 보조계류시스템; Ice load 빙하중; Heading control 방향제어; Position control 위치제어;

Chapter 1. Introduction

1.1 Background

Since the continuous demands of oil and gas, it is expected to develop regions of severe condition such as deep sea and Arctic ocean. Especially, various efforts have been made to develop oil and gas in the Artic ocean. The presence of ice load in Arctic ocean is one of the critical factors which makes the floating offshore platforms be difficult to keep their position and heading. Station keeping of floating platforms is normally achieved by three type of systems which are mooring system, DP system and DP assisted mooring system. Mooring system enables the station keeping using multiple lines connected on platform and seabed. DP system achieves the station keeping using several thrusters which can counteract environmental load. DP assisted mooring system which combines both systems is used to decrease the weight of mooring system in the sea of deep depth or when the high performance of station keeping is required. Especially in Arctic ocean, DP assisted mooring system can be a reasonable solution for safety operation of permanent production platforms(Ryu and Kim, 2003). The control strategy of DP assisted mooring system is normally performed using position control from mooring system and heading control from DP system in normal condition. However, the position control of DP system should be conducted when the continuous increase of mooring tension is occurred even if the mooring system is utilized with maximum capacity. And also, the heading control of DP system is important especially in Arctic ocean. In normal sea, the most stable heading of platform can be achieved naturally by weather-vaning. However, the proper heading which can minimize loads from ice should be calculated by DP controller in Arctic ocean since the ice-vaning is not performed naturally.

For this reason, this thesis is focusing on methods to control position and heading of platform applying DP assisted mooring system in Arctic ocean. The new position and heading control strategy considering real time tension is suggested for the objective of safe and fuel-effective operation.

1.2 Literature Review

The research about station-keeping for floating offshore structure is active in the world. DYPIC project which is completed within 2012 conducted model test with DP under ice condition and validated the feasibility of DP in various ice conditions(Jenssen et al., 2012). Liferov et al. (2018) performed SKT project which is worked at 6 locations of Arctic Ocean to test ice management techniques, performance of DP and various control strategy. DP control under ice condition is obviously different with open water because of various ice effect. In terms of control of DP system, the compensation for surge and sway of DP assisted mooring system is normally performed by mooring system for objective of fuel-effective operation. Meanwhile, DP system provides yaw moment using heading control(Strand, 1999). However, in severe condition, DP should control not only heading but also positions to keep the tension of mooring system within limited ranges(Strand et al., 1998). The control for tension reduction can be made using SP(Set Point) control which automatically calculates the specific position. Berntsen et al. (2008) suggested SP control method using reliability index of mooring lines. The reliability index which quantifies the probability of mooring line failure is calculated according the time varying weather condition and finally SP is produced utilizing calculated reliability index. Nhuyen and Sorensen (2009) generated SP with respect to the level of environmental condition. When the extreme condition, SP is calculated closely to the field zero position where the equilibrium position of the moored vessel when there is no environmental loads to prevent breakage. At turret mooring in normal environmental condition, especially, heading control of DP assisted mooring system can be naturally performed by weather-vaning in normal condition. However, under ice condition, DP is required to align heading of platform with ice drift direction to minimize loads from ice. Zhou et al. (2013) conducted numerical simulations to validate effects of heading control under ice condition. The test with heading control towards ice drift direction satisfied the reduction of mooring loads and drift. Kerkeni and Metrikin (2013) emphasized the necessity of heading control for operation with DP system under ice condition. And Automatic heading control against ice drift direction is suggested. They suggested that if the platform is with mooring system, an automatic heading control considering tension is required certainly. Kerkeni et al. (2018) performed the full scale test with DP system in Arctic ocean. The heading control with control laws for normal sea failed the station-keeping. Manual control with DPO(Dynamic Positioning Operator) and heading control for ice condition are emphasized. From the various research, it is essential to control heading towards ice drift direction to prevent the failure of mooring system and for saving cost of ice-breaking vessel under ice condition.

1.3 Contents of Thesis

In order to introduce thesis, Chapter 1 focuses on the objective, previous and summary of research. The new position control for DP assisted mooring system is developed in Chapter 2. Then, the capability analysis of DP system in various ice condition is conducted in Chapter 3 to analyze the characteristics of ice parameter. Chapter 4 suggested the new heading control method in Arctic ocean. And also, the total control strategy containing position control in Chapter 2 and heading control are simulated under ice condition. Chapter 5 summarized the work flow of thesis and concluded the result.

Chapter 2. Position control

2.1 Overview

Chapter 2 is focusing on the development of new position control strategy for DP assisted mooring system in normal and Arctic ocean.

In this thesis, the method for tension estimation around platform in real time is suggested to generate SP as a position control strategy. In order to estimate tension, a local tension estimation considering tension of real-time and a global tension using static analysis results of mooring system are combined. Finally, a position representing a minimal tension estimation is selected as a SP.

2.2 Local tension estimation

2.2.1 Objective

For the position control which can keep the platform and mooring system in safety range, SP should be determined to the direction of tension reduction. In this thesis, a strategy for tension estimation around current platform position is suggested for determining SP which can reduce tension. Tension estimation is conducted by combination of two components : A local tension estimation and a global tension.

Firstly, in this paragraph, a local tension estimation method is introduced. The local tension estimation is a process of estimating the tension distribution in the area around the current platform by using the variation of tension due to the position change of platform during the recent time. In other words, local tension estimation includes tendency of recent tension variation. Using the local tension estimation, tension increase or decrease areas can be specified and mainly directionality for SP determination is presented.

2.2.2 Generation of grid

The local tension estimation is conducted at limited area named 'Local grid'. In the process of tension estimation, the activity area of the platform is represented by a grid, which is used to perform fast calculations by restricting many positions that can be selected by SP. Therefore, SP would be determined in one position of grid.

There are two types of grid : A global grid and a local grid. The global grid which is shown as solid line in Fig. 1 is built around initial position of platform when there is no environmental loads. The global grid is always fixed regardless of position change. Position of platform can be represented applying the x and y coordinate system which the horizontal position is x and the vertical position is y. The local grid is shown as slash line in Fig. 1. The local grid is a grid that is built around the current location of the moving platform and updated as it moves.

Two types of grid sizes is set considering the offset of the mooring system. It is to limit the position that can be selected as SP in the range of the offset so that the position control can prevent excessive tension rising in advance.

2.2.3 Estimation process

The local tension estimation is conducted by using recent position and tension tendency. Therefore, the current position is defined as Eq (1) and current tension of all mooring lines is defined as Eq (2). Eq (3) is past position and Eq (4) is tension of all mooring line in past time. The past time can be determined considering fluctuation of tension. The local tension is estimated based on the variation of past and current data so that variation of position and tension is defined at Eq (5) and (6).

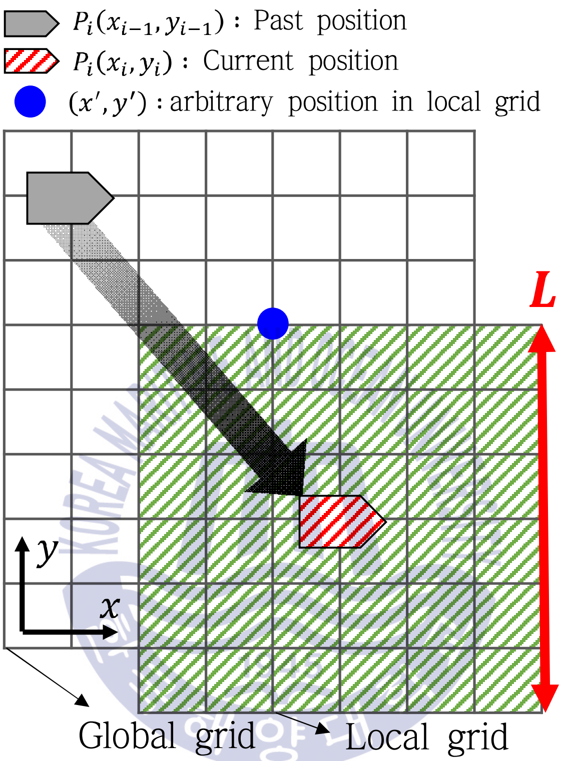

Fig. 1 Configuration of local and global grid

$$P_i = (x_i, y_i)\ (i = time\ instance) \tag{1}$$

$$P_{i-1} = (x_{i-1}, y_{i-1}) \tag{2}$$

$$T_i = [T_1, T_2, \cdots\ T_n]^T (n = The\ number\ of\ mooring\ lines) \tag{3}$$

$$T_{i-1} = [T_1, T_2, \cdots\ T_n]^T \tag{4}$$

$$\begin{Bmatrix} \triangle x = x_i - x_{i-1} \\ \triangle y = y_i - y_{i-1} \end{Bmatrix} \tag{5}$$

$$\triangle T_n = (T_n)_i - (T_n)_{i-1} \tag{6}$$

Assuming that the tension variation of the mooring system about the platform movement is linear, Eq (7) can be defined as the unit tension variation per distance from the past position to the current position.

Based on unit tension variation, Eq (7), the tension at each coordinate of the local grid can be estimated by multiplying the deviation of local grid coordinate and past structure position to the unit tension variation as shown Eq (9).

Specifically, assuming arbitrary coordinate of the local grid as (x', y') specified as a point in Fig. 1, the deviation of past position and each local grid coordinate can be calculated by Eq (8). Using this $(\triangle x', \triangle y')$ which is position deviation and unit tension variation, estimated tension at arbitrary coordinate of local grid can be calculated by multiplying two values with Eq (9).

The result of Eq (7)~(9) calculation is tension of horizontal and vertical direction for each line at one coordinate of local grid. In order to compare estimated tension with all coordinate of local grid, horizontal and vertical tension is summed with Eq (10) for each lines. Through Eq (10), tension maintaining directionality can be generated.

Eq (10) is tension estimation for only one line of mooring system. Since mooring system is normally composed as various lines, Eq (7)~(10) is needed to repeat with respect to the number of mooring lines. In this case, the number of estimated tension would be the number of lines. Finally, estimated tension of all lines are summed by Eq (11).

The objective of SP control is to determine SP considering safe production which enables fuel-efficient operation not in survival condition. For that reason, It is considerable to determine SP where can reduce the tension of entire mooring system, not a single mooring line. With consideration of this objective, the summed local tension estimation is able to be calculated at one coordinate of local grid following Eq (7)~(11).

$$(Unit\ T_x)_n = \frac{\triangle T_n}{\triangle x},\ (Unit\ T_y)_n = \frac{\triangle T_n}{\triangle y} \tag{7}$$

$$(\triangle x', \triangle y') = (x' - x_{i-1}, y' - y_{i-1}) \tag{8}$$

$$(T_x, T_y)_n' = ((Unit\ \ T_x)_n \times \triangle x', (Unit\ T_y)_n \times \triangle y') \tag{9}$$

$$(T_n)' = (T_x)_n' + (T_y)_n' \tag{10}$$

$$T = \sum_{n=1}^{\substack{The\ nummber\ of \\ mooring\ lines}} (T_n)' \tag{11}$$

2.2.4 FPSO with mooring system for a simulation

In order to perform a simulation to determine the SP, the process of local tension estimation is firstly performed. The model platform used in the simulation is FPSO(Floating Production Storage Offloading) and the principle dimension is specified in Table 1. The vessel’s geometry is shown in Fig. 2. Mooring system is turret and catenary type and the configuration is shown as

Fig. 3. Turret is located 50m away from the center of the ship to bow.

Table 1 Main dimension of model structure for simulation

Principal dimension	Value
Length between perpendiculars(LBP) [m]	244
Breadth [m]	50
Draft [m]	18.6
Displacement [m3]	163215
GM [m]	4.43
Vertical center of gravity(VCG) [m]	18.5
Radius of gyration for x [m]	15.2
Radius of gyration for y [m]	59.3
Radius of gyration for z [m]	60.0

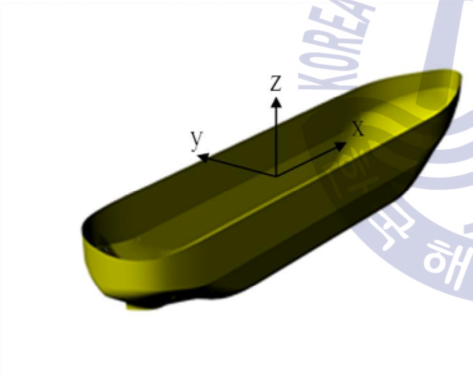

Fig. 2 Geometry of model vessel

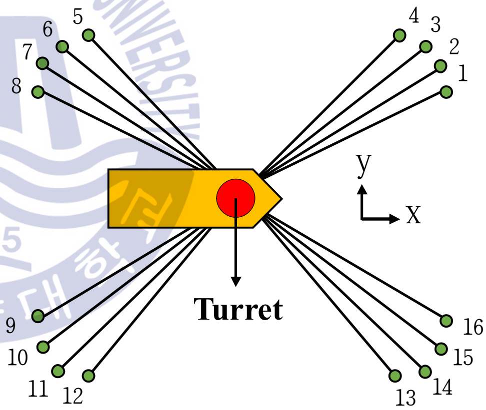

Fig. 3 Configuration of mooring system

2.2.5 Local tension calculation

For the local tension estimation, position and tension data are generated through 3 hours motion analysis of platform and mooring system in wave, wind, and current condition. From the result of motion analysis, time history of surge, sway position and tension of all mooring lines are generated as shown Fig. 4. Especially, tension time history is filtered by low pass filter to consider low frequency effect only. Based on Eq (1) and (2), $i-1$ is 9110s data and i is selected 9120s which has interval of 10 seconds considering the section where the tendency of tension increase or decrease can be maintained. Selected position and tension at 9110s and 9120s are specified in Table 2.

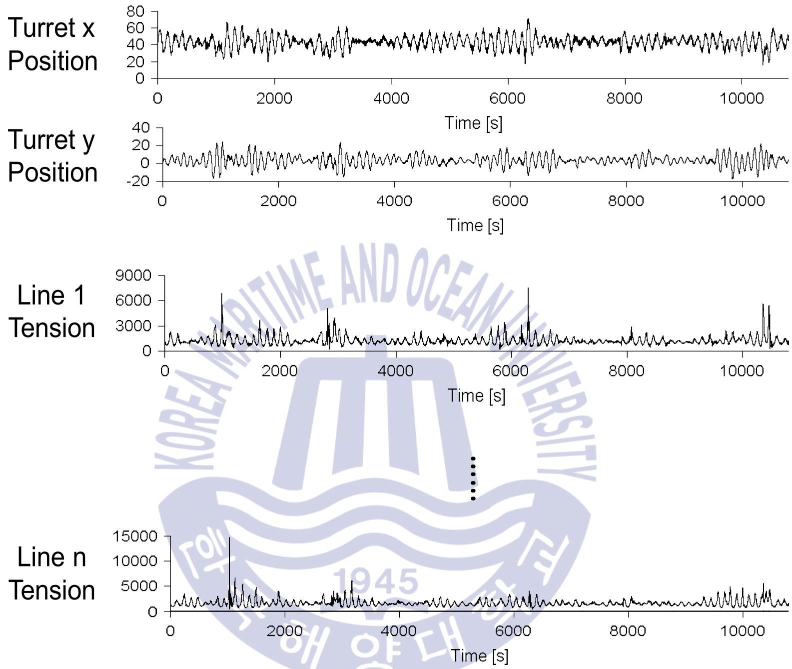

Fig. 4 Result of platform and mooring analysis by Orcaflex

Table 2 9110 and 9120s data for local tension estimation

Time		9110s (t=i-1)	9120s (t=i)
Position [m]	x	46	49
	y	21	2
Tension [kN]	Line 1	504	1114
	Line 2	506	1107
	Line 3	508	1100
	Line 4	511	1093
	Line 5	708	984
	Line 6	716	986
	Line 7	725	988
	Line 8	734	989
	Line 9	2203	1172
	Line 10	2263	1178
	Line 11	2203	1172
	Line 12	2385	1188
	Line 13	1870	1267
	Line 14	1792	1267
	Line 15	1715	1266
	Line 16	1641	1265

The size of local grid for local tension estimation is set based on offset of mooring system. As preventing platforms from escaping the mooring offset, the SP is determined within the range of permissible tension and also fuel-efficiency and safety in terms of operation can be expected. The offset of catenary mooring system is normally 10~20% of water depth. The depth used in this simulation is 150m and then offset is 15 ~ 30m. Therefore, the length of the side of the local grid specified in Fig. 1 is set at 60m considering the radius of maximum offset, 30m. Finally, the total size of the local grid is built by 60 X 60 m^2 centering on the turret position.

According from Eq (7) to Eq (11), estimated local tension for each position of local grid is represented by the z-axis of Fig. 5 and is schematized into a 3-dimensional graph. From the Fig. 5, The direction of tension increase and decrease can be seen around the platform position of 9120 seconds which is (49,2). Consequently, the local tension estimation can be applied to determine the direction of the control considering the recent tension change trend when calculating the SP.

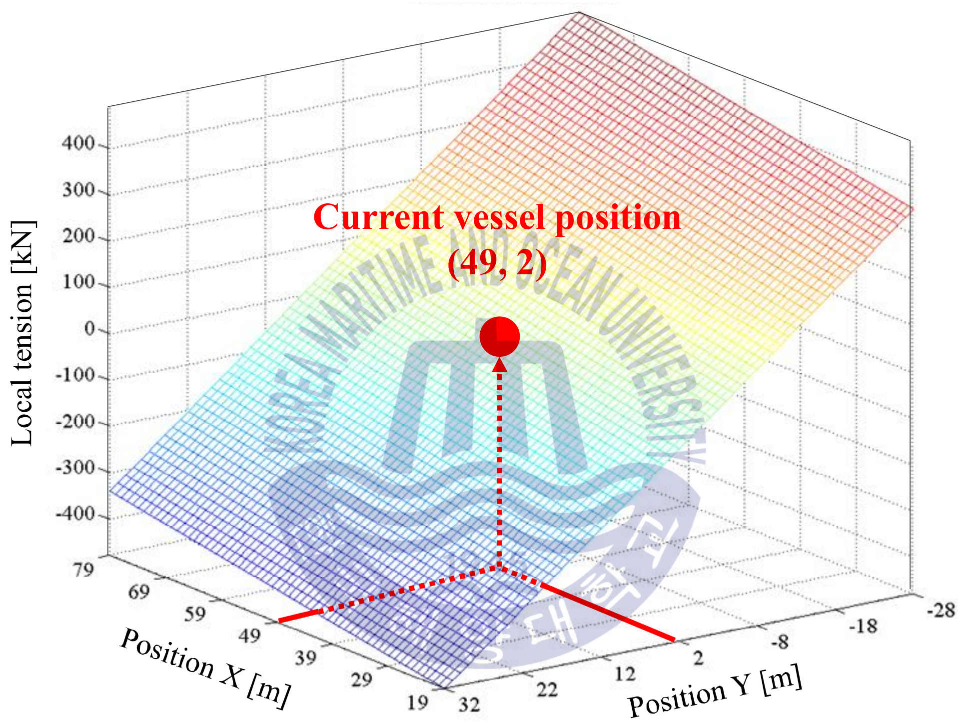

Fig. 5 Result of local tension estimation

2.3 Global tension generation

2.3.1 Objective

Global tension is calculated based on global grid and is a tension calculated at offline unlike local tension through static analysis of platform and mooring system. The global tension is an component with local tension that is included to determine SP. The global tension includes the load distribution of the mooring system according to the movement of the platform so that areas where excessive tension occurs can be intuitively specified and also important information for determination of control direction. With the process of local tension estimation, the global tension is also generated for simulation of SP calculation.

2.3.2 Calculation of global tension

Global tension is obtained from the same ship which is specified in Table 1 and mooring system which is specified in Fig. 3 as local tension.

The global tension is generated through static analysis of platform and mooring system. The structure and mooring system at the initial position without environmental loads are moved to each coordinate of the global grid as shown Fig. 6 and the tension for each coordinate is calculated through static analysis. Since the mooring system used is symmetrical around the turret, only the first quadrant is static analysis and symmetrically assumed the tension of the remaining part.

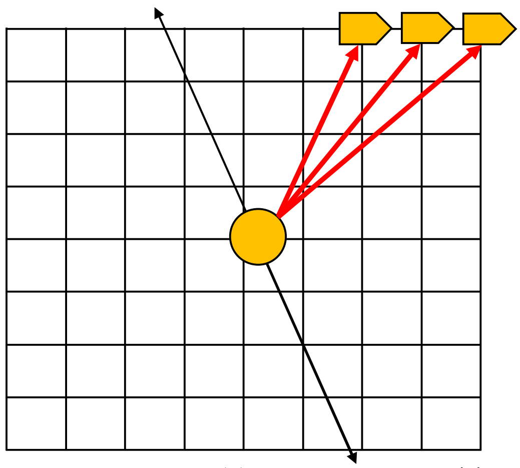

Fig. 6 Process of global tension calculation

From the result of static analysis at all coordinate, tensions of 16 mooring lines are generated. As with the purpose of the local tension estimation, the global tension is also considered for determining the SP for increasing the performance of production operation. Therefore, since the SP should be determined to reduce the overall tension of the mooring system, tension of all mooring lines are combined to be used as global tensions. The calculated global tension is represented on the z-axis of the grid and represented by a 3D graph as Fig. 7. From the result graph, the area of excessive tension can be intuitively judged when moving the platform, and the tension variation characteristics of the mooring system according to the control direction can be included in the SP calculation algorithm.

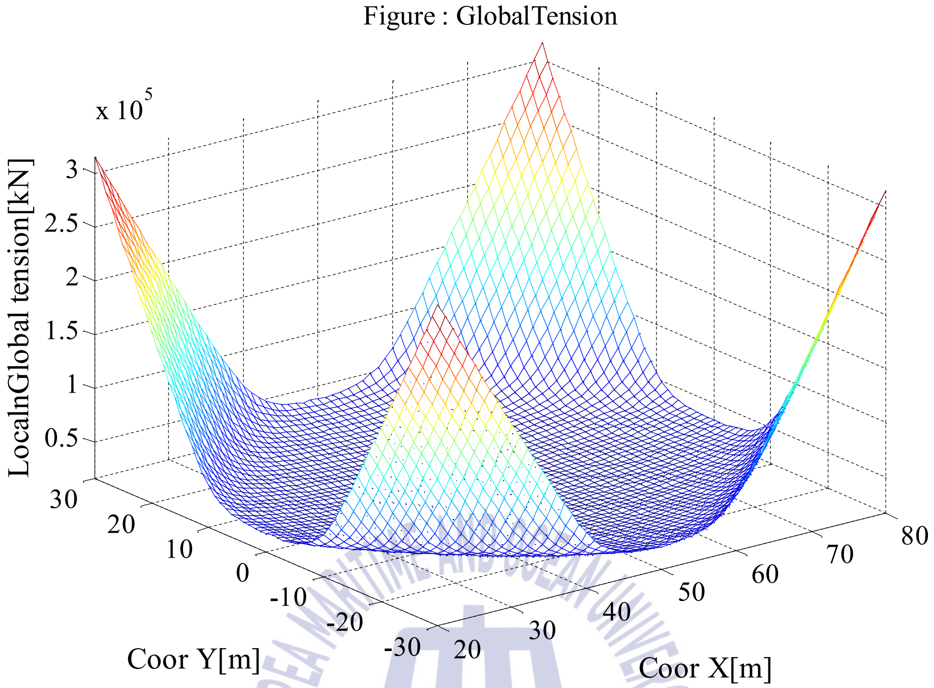

Fig. 7 Global tension on global grid

2.4 Determination of SP

Finally, in order to select SP that satisfies the prevention of excessive drift and tension increase, superposition of local tension estimation and global tension for the SP determination is conducted. And also, calculation of SP is performed through simulation.

2.4.1 Superposition of local and global tension

In order to determine SP, superposition of local and global tension is required to consider both components. Superposition can be conducted at overlapped area of local and global tension as shown shading area in Fig. 8. In this area, the local and global tension at each overlapped coordinate are summed by Eq (12) with having certain ratio.

Certain ratio called 'α' can be calculated by Eq (13) and α is different for each coordinate of overlapped area. α is applied to sum the local and global tension with different ratio for each coordinate. As far from the current position of platform, the shape change of mooring line and the dynamic elements of environmental load will increase. Therefore, the local tension estimation method which assumed the mooring as linear system may not proper to estimate tension. From that reason, the global tension is remarkable component than local tension at far coordinate from current position.

Therefore, α is a weight factor to focus on the weight of global tension depending on the distance. α is specified as ratio of the coordinate from center of local grid to the maximum diagonal length of the local grid as shown Eq (13). That is, ratio of dot line to solid line in Fig. 8.

$$\text{Superposed tension} = (1-\alpha)Local\,tension + \alpha\,Global\,tension \tag{12}$$

$$\alpha = \frac{\sqrt{(x^{'}-x_i)^2+(y^{'}-y_i)^2}}{\sqrt{(\frac{L}{2})^2+(\frac{L}{2})^2}} \tag{13}$$

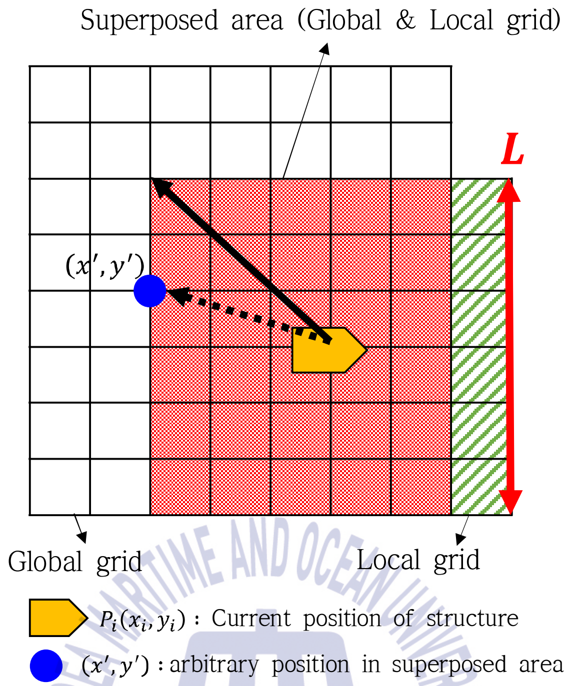

Fig. 8 Process of superposition

Finally, SP is determined minium tension estimation in overlapped area. Superposed tension estimation is specified as z-axis of Fig. 9. Fig. 9 shows only overlapped area and the solid point is SP at 9120s which has the lowest tension estimation. At 9120s, the current position and SP is same as (49, 2) since the current position is already close to equilibrium position of platform when there is no environmental loads.

2.4.2 Result of SP

3 hours DP and mooring simulation is performed to verify that the calculated SP is set in a reasonable direction at real time. The simulation is conducted by Orcaflex which is a time domain analysis software. The platform

and mooring system is same with data of paragraph 2.2.4. Configuration of DP system is specified in Table 3. Environmental condition used for simulation is specified in Table 4.

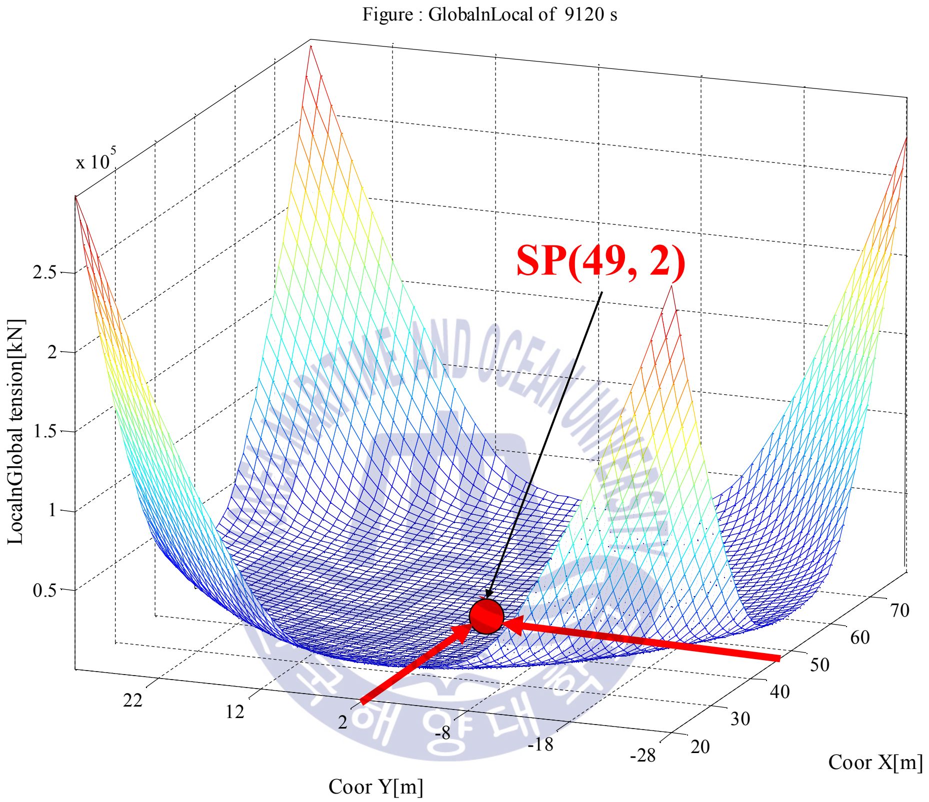

Fig. 9 Overlapped area of global and local tension

Table 3 Principle dimension of actuators and arrangement

No.	Type of thruster	Thrust [kN]	Thruster arrangement
1	Tunnel thruster	330	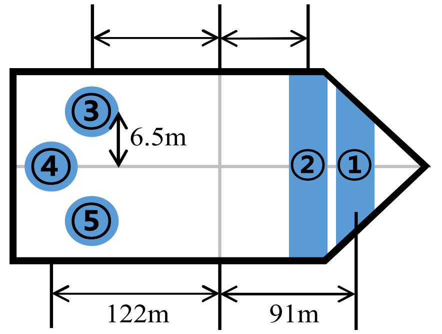
2	Tunnel thruster	330	
3	Azimuth thruster	875	
4	Azimuth thruster	875	
5	Azimuth thruster	875	

Table 4 Environmental condition for simulation

	Wave	Wind	Current
Properties	JONSWAP spectrum $H_s = 10.06\,m$ $Tz = 11.63s$	NPD spectrum $V_w = 22.54\,m/s$ $Elevation\ = 10m$	Steady condition $V_c = 0.3\,m/s$
Direction	180 degree	150 degree	135 degree

Since mooring system used for this simulation is internal turret, 3 azimuth thrusters are arranged at astern and 2 side thrusters are arranged at bow.

During the simulation, DP system is activated and SP is determined when the position of platform is over the boundary condition. Otherwise, the position control is conducted by mooring system only. The boundary condition is 2 types. Firstly, when the platform is over the 50% of mooring offset. Secondly, when the maximum tension of mooring lines is over the 50% of M.B.L(Minium Breaking Load). If either of these conditions is satisfied, the DP system will be activated and SP for position control would be determined.

From the determined SP, PD controller of DP system calculates required thrust to arrive at the SP. The gain for P is calculated considering natural period of surge which is about 90 seconds at mooring system. D gain is determined as 50% of critical damping of mooring system. Gain values are specified in Table 5.

Table 5 PD gain for simulation

	P gain	D gain
surge	8.8×10^5	1.2×10^6
sway	1.5×10^5	1.6×10^6
yaw	2.25×10^9	1.0×10^{10}

2.5 Result of position control

During the 3 hours simulation, Determination of SP is conducted 71 times since the platform exceeded the boundary condition of 71 times. Fig. 10 represents the platform's position and calculated SP when the platform exceeds the boundary condition which is a 50% of maximum mooring offset. Almost SP is determined as close to initial position which is the position of (50, 0). The initial position means that the most stable position regarding to mooring system. Therefore, the SPs are calculated to the direction satisfying reduction of tension.

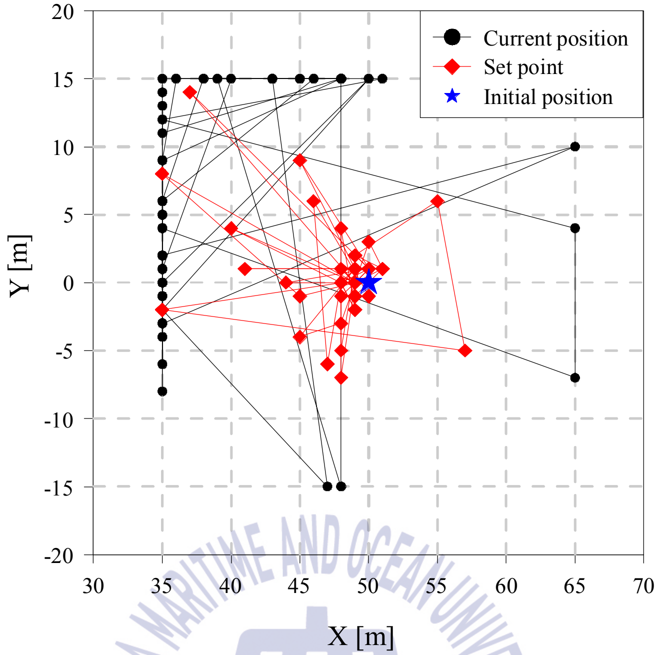

Fig. 10 Calculated SP and current position during 3h

Results from the (a) of Fig. 11 to (d) of Fig. 11 show the tension of mooring according to the control of the DP with calculated SP during 3h simulation. The tension of lines which the environmental loads acts on the most are represented as a result. From the result, the tension with DP control shows lower maximum value than the tension without control. especially, the tension of about 1100 seconds is reduced by up to 63% due to control. As a result, the calculated SP for position control prevents the excessive tension increase.

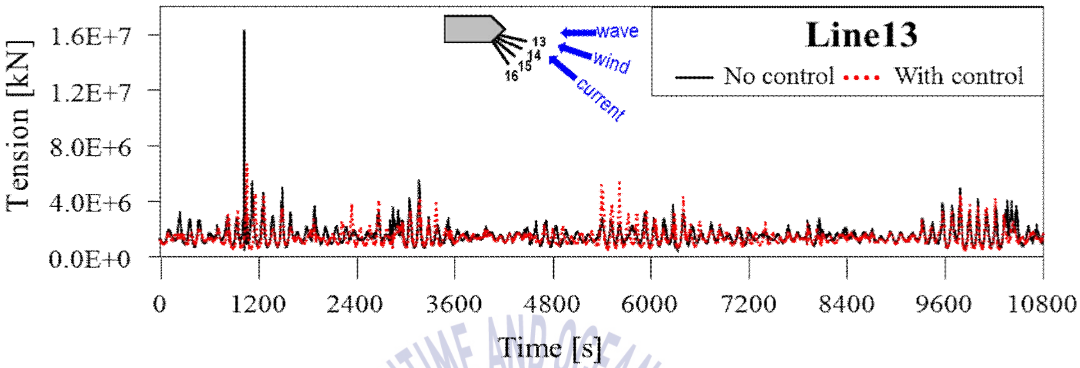

Line13
No control
With control
wave
wind
current
13
14
15
16
Tension [kN]
1.6E+7
1.2E+7
8.0E+6
4.0E+6
0.0E+0
0
1200
2400
3600
4800
6000
7200
8400
9600
10800
Time [s]

(a)

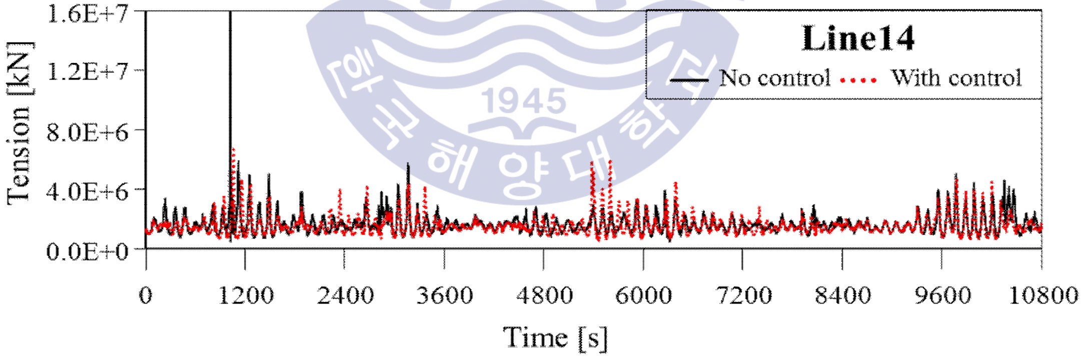

Line14
No control
With control
Tension [kN]
1.6E+7
1.2E+7
8.0E+6
4.0E+6
0.0E+0
0
1200
2400
3600
4800
6000
7200
8400
9600
10800
Time [s]

(b)

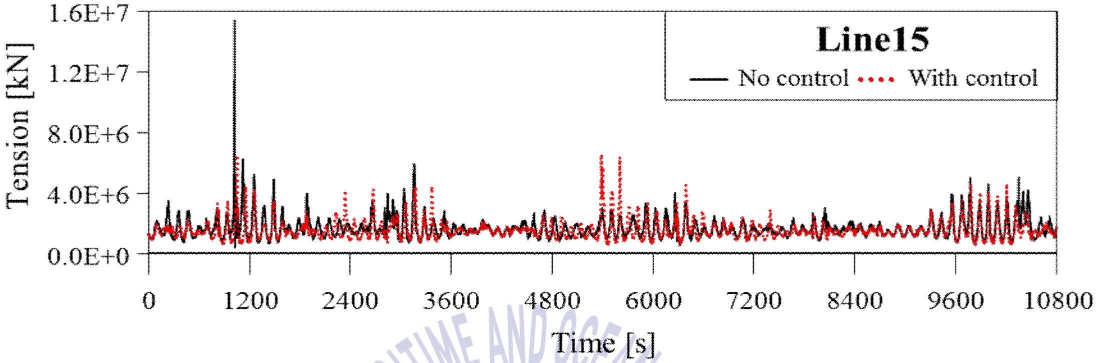

(c)

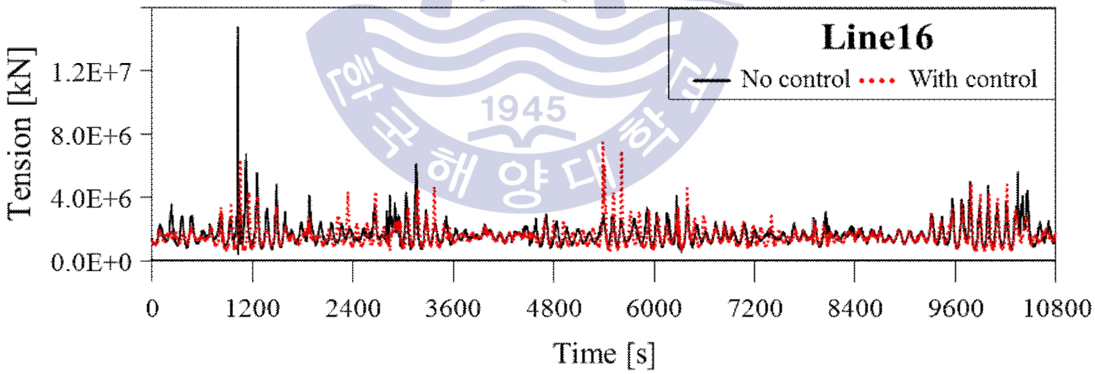

(d)

Fig. 11 Tension of 13, 14, 15 and 16 line during 3h simulation

Fig. 12 is the result of showing the average of the most and second loaded mooring lines from the result of 3 hours simulation. The range marked by the shade is the range where the SP is calculated and the control of DP is activated because the platform corresponds to the boundary condition. Especially, the tension of 2500~3000s and 5000~5500s is represented in Fig. 12. The result shows a decrease in tension in most shaded sections when the DP control starts. Therefore, It is validated that the SP is determined to a direction that satisfies the reduction of the tension.

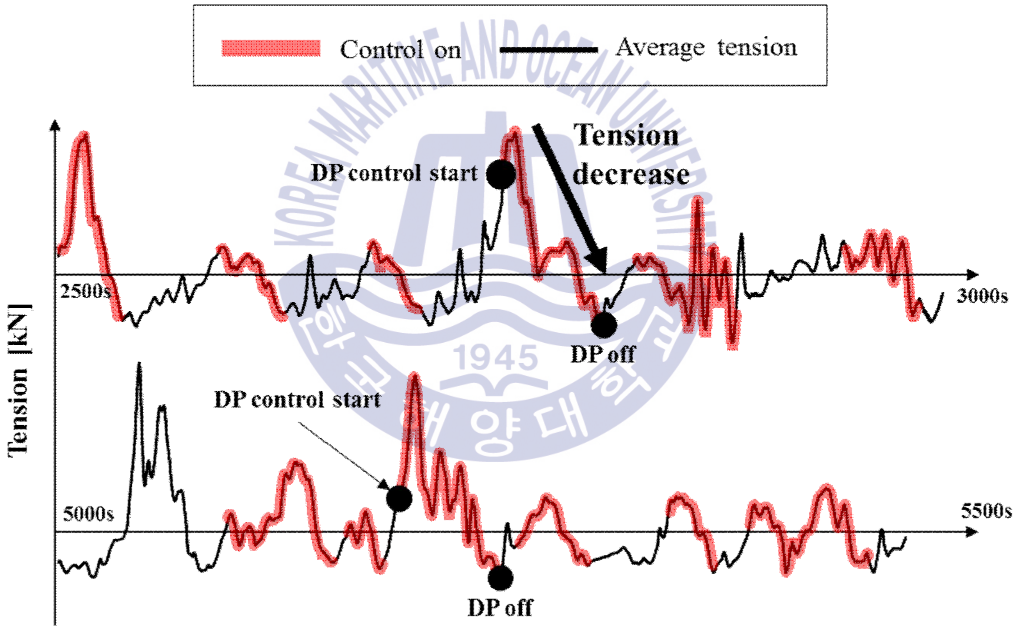

Fig. 12 Average tension of the 1^{st} and 2^{nd} loaded line with respect to time

From the results, It is validated that the new strategy produces SP which can reduce the total tension of mooring system reflecting tension variation of recent time. The variation interval of tension is determined as 10 seconds in this study considering the response of mooring tension by wave frequency. It is very important to set tension interval when the response of high frequency has extreme fluctuation.

Furthermore, SPs are determined to the directions which prevent the increase of tension. These SPs has direction close to initial position but are not determined to initial position. In terms of global perspective, the most stable position is initial position and it can be considered proper SP. However, if the real-time state of position and tension is not considered, considerable and unnecessary fuel consumption can be occurred to arrive at initial position. Also, since DP assisted mooring system for production platform is required to control position within the wider boundary than drilling platform, it is appropriate to control for reducing the failure by reflecting the current state rather than excessive control to the initial position for fuel-efficient production operation.

In summary, 3 conclusions of this chapter are introduced as below.

(1) The strategy using tension estimation has good agreement with the direction where enables the reduction of tension.

(2) It is important to optimize tension interval to reflect tension variation for SP determination.

(3) It is appropriate to control with strategy of determining SP suggested by this study for fuel-efficient production operation.

Chapter 3. DP capability analysis under ice condition

3.1 Overview

Chapter 3 is focusing on the procedure of DP capability analysis including ice and the results of analysis according ice parameters.

In the stage of design, it is very important to analyze the capability of DP system for floating structures in given environmental condition. Typically, the capability of DP system can be evaluated through 2 methods : Static analysis using DP capability plot, Dynamic analysis using time simulation. Static analysis is conducted to calculate the limitation of environmental condition which the designed thruster configuration and capability can keep the position. From the result of static analysis, DP capability plots which is a type of polar graph are produced as shown Fig. 13. DP capability plots have been used at the initial stage of design since it has simple and fast calculation process than time simulation. Also, this result can be utilized for the direct comparison of various DP system and also for DP operator.

In normal environmental condition, DP capability plot can be produced including wave, current and wind load. However, the ice loads should be considered for capability analysis of DP system in Arctic ocean. In order to design DP system in Arctic ocean, sensitive and influential ice parameters should be organized. Especially, in order to develop the control strategy of DP assisted mooring system in Arctic ocean, the ice characteristics and the permissible range which DP system can stay should be analyzed.

3.2 DP capability plot without ice loads

There are many types of capability plot such as wind envelope and thrust envelope with respect to the objectives. However, all DP capability plots are generally calculated following the standard specification of IMCA(International Marine Contractors Association) (IMCA, 2000). IMCA suggested the process to calculate various capability plots. The calculation process can be different slightly depending on the type of capability plot. However, All calculation is based on the specification of IMCA. In this thesis, wind envelope and thrust envelope which are the most widely used type is introduced and generated.

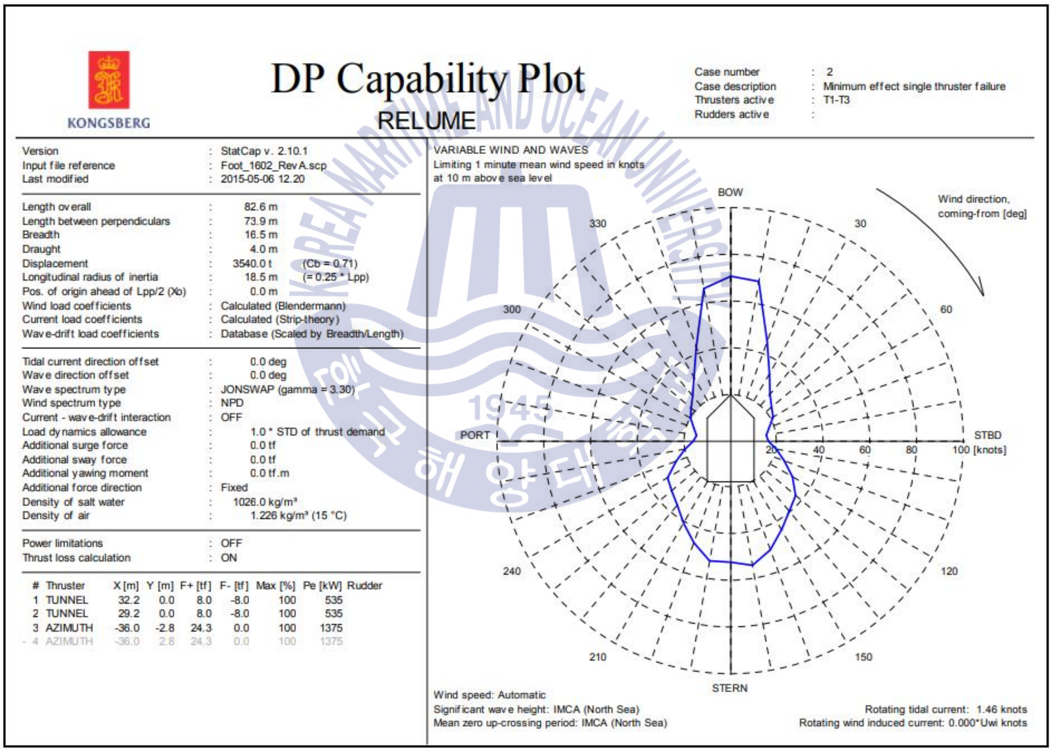

Fig. 13 Example of DP capability plot (Kongsberg, 2015)

3.2.1 Wind envelop

Wind envelope represents the maximum wind speed which the DP system can keep the station in given environmental condition. Since wind is unpredictable and the most influential component to make wave, DP capacity should be determined considering the wind force(최진우 et al. 2012). Fig. 14 is a procedure for calculating the wind envelope. Firstly, range and interval of wind speed to evaluate DP capability is required. Normally, maximum wind speed is 50 m/s and the interval is determined as 2.5 m/s according to IMCA. Secondly, wind, wave and current forces are calculated at one direction and based on one wind speed. Wind and current forces can be calculated using coefficient and projection area. And the properties to calculate wave force is determined using Table 4. With respect to Eq (14) suggested by IMCA, Summation of all forces represents the required thrust of DP system to encounter environmental loads. $\overrightarrow{F_{wi}}$ is wind force, $\overrightarrow{F_{wa}}$ is wave force, $\overrightarrow{F_{cu}}$ is current force and $\overrightarrow{F_{th}}$ is required thrust to encounter the summation of wind, wave and current environmental loads. In order to consider the limitation of thrusters, the required thrust is distributed at the stage of thruster allocation. The distributed thrust is re-summed for comparison with available thrust of given DP system. Depending on the iteration process of Fig. 14, calculation is repeated with increasing wind speed if the available thrust is enough than required thrust. On the other hand, if the required thrust is over the available thrust of DP system, the wind speed is determined as the maximum speed which the DP system can stay the station at the direction. This speed is specified on the wind envelope. Finally, Wind envelope can be produced repeating the calculation process with respect to all environmental direction.

$$0 = \overrightarrow{F_{th}} + \overrightarrow{F_{wi}} + \overrightarrow{F_{wa}} + \overrightarrow{F_{cu}} \tag{14}$$

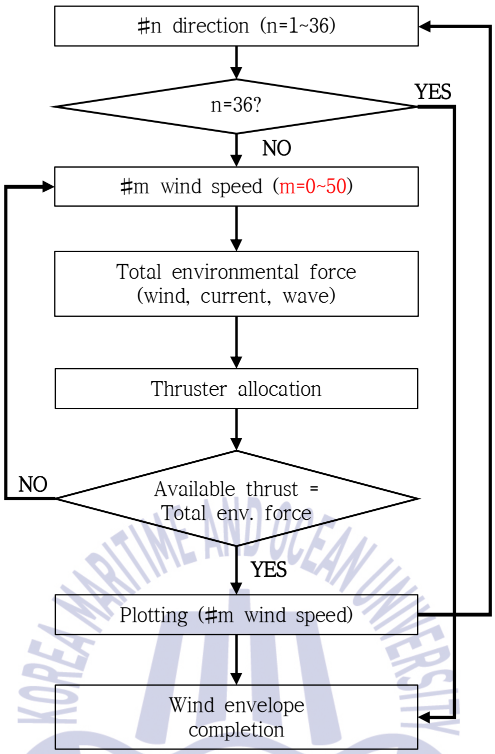

Fig. 14 Generation procedure of wind envelop

3.2.2 Thrust envelop

Thrust envelope represents the maximum ratio of required thrust to available thrust for each thruster in given environmental condition. In other words, thrust envelope indicates the margin of available thrust for each environmental direction. Thrust envelope may be calculated following Fig. 15. Unlike wind envelop, thrust envelop needs one wind speed. For each environmental direction, wind with one speed, current and wave is calculated. Total environmental forces which is required thrust are distributed at the stage of thruster allocation. Distributed thrust is compared with available thrust for each thruster. Then, the most maximum ratio is recorded on thrust envelope. Finally, thrust envelope can be produced with repeating this process with respect to the number of environmental directions

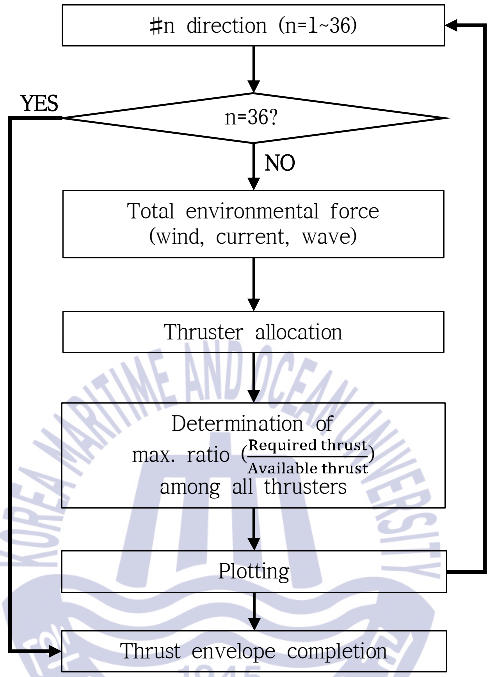

Fig. 15 Generation procedure of thrust envelop

3.3 DP capability plot under ice condition

3.3.1 Overview

In order to generate the DP capability plot under ice condition, the ice load should be added to Eq (14) which is the original method in normal condition. Eq (15) includes the ice load $\overrightarrow{F_{ice}}$. In this thesis, DP capability plot under ice condition is produced by Eq (15) considering various ice parameters.

$$0 = \overrightarrow{F_{th}} + \overrightarrow{F_{wi}} + \overrightarrow{F_{wa}} + \overrightarrow{F_{cu}} + \overrightarrow{F_{ice}} \qquad (15)$$

3.3.2 Characteristics of ice load

3.3.2.1 GEM simulator

The ice load is calculated using GEM(GPU-Event-Mechanics) simulator. GEM is a new numerical analysis method suggested by ABS(American Bureau of Shipping) and Memorial university for prediction of vessel navigation path(Daleyet et al., 2012). GEM enables the fast and huge computation of many ice floes simultaneously using GPU hardware, a processor dedicated to graphics operation. In the simulator, various ice floes can be modelled as 2D feature of polygon like Fig. 16(a). And also, many options such as floe sizes and concentration can be randomly distributed or set depending on user like Fig. 16(b). When the impact between vessel and every ice floe is occurred, the ice load is recorded.

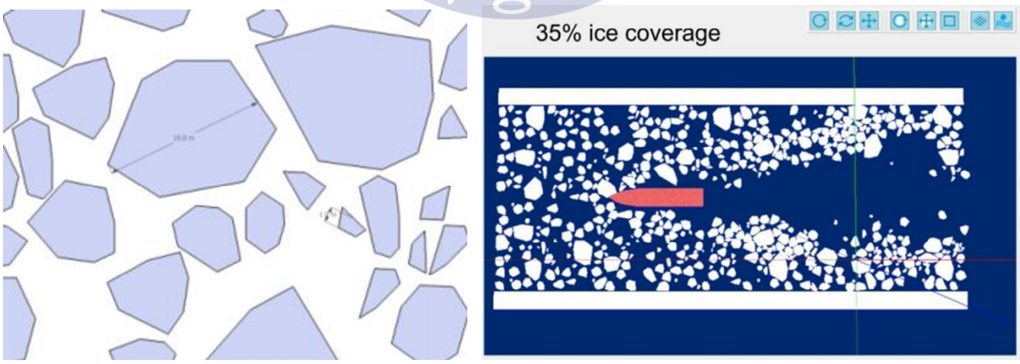

(a) (b)

Fig. 16 2D geometry of ice floe in GEM simulator (Daley et al., 2014)

3.3.2.2 Ice parameters

Ice parameters for calculation of ice load is analyzed using previous research. It is important to consider major ice parameter affecting DP operation. ITTC guideline introduces list of ice parameters for model test under ice condition and also main parameters(ITTC, 1999). DYPIC project which develops a new DP simulator under ice condition suggested major ice parameters applied to towing experiment(Jenssen et al., 2012). Generally, ice parameters used for model test and simulation are ice concentration, size, thickness, density, drift velocity and drift direction. Priority of parameters can be different with respect to test condition and objective of test. In this thesis, ice concentration, thickness, density, velocity and crushing strength are selected for analyzing of DP capability. The crushing strength is one of the major ice parameter considered in simulation of DP vessel and ice collision(Nguyen et al., 2009). Specific condition of ice parameter is selected as shown in Table 6 based on the ice data of target sea. The target sea is Chukchi sea which is one of the areas of ARC7 ice class classified by RMRS(Russia Maritime Register of Shipping) (RMRS, 2016). 1-year ice thickness of ARC7 ice class is about 1.7m in summer and autumn. In spring and winter, about 1.4m is a ice thickness(RMRS, 2016). Considering this information, the thickness condition is selected as 1.0, 1.5 and 2.0m. Ice drift velocity is selected using current velocity of Chukchi sea. 10,000 year period current in Chukchi sea is around 0.3~0.9m/s(Jung et al., 2017). Therefore, the ice drift velocity condition is selected as 0.5, 0.8, 0.9 and 1.0 m/s. The ice crush strength and density are selected by using the data of general drift ice around world since these parameters vary considerably depending on seas and seasons. The ice crushing strength is selected as 1.8, 2.0 and 2.2MPa. Ice density is chosen consdering sea density(1025kg/m^3) and ice density(920kg/m^3). Selected ice density condition is 850, 900 and 950kg/m^3.

Table 6 Principal ice parameters for simulation

Ice parameter	Value
Ice concentration [%]	80 (Fixed)
Ice thickness [m]	1.0, 1.5, 2.0
Ice drift speed [m/s]	0.5, 0.8, 0.9, 1.0
Ice crushing strength [MPa]	1.8, 2.0, 2.2
Ice density [kg/m^3]	850, 900, 950

3.3.2.3 GEM simulation for ice load

The model vessel for DP capability analysis is FPSO(Floating Production Storage Offloading) which is production platform. The principal dimension is represented in Table 1. Fig. 2 is model vessel. Thrusters are specified in Table 3.

Using selected ice parameters, the ice load for DP capability analysis is calculated by GEM simulator. Mixing conditions in Table 6, simulation cases for GEM are generated in Table 7. The ice floe size is produced randomly in the range of 10~50m. In GEM simulation, the ice drift direction is considered fixing ice drift direction and changing Yaw angle of vessel from 0 degree to 50 degree with the interval of 10 degree. Fig. 17 shows rotated angle of vessel. Rotated vessel drifts to the area of ice and the ice load would be generated as time history like Fig. 18 (Han et al., 2017). The final ice load to calculate DP capability plot is mean value considering stable range of ice load. After conflict between the vessel and ice, ice load increases continuedly. If the vessel is fully affected by the ice zone, the ice load fluctuates precipitously but with a constant mean value. When the vessel begins to drift out of the ice zone, ice loads tend to decrease. Consequently, mean ice load is computed at stable range except increase and decrease region in time history. Ice loads are generated in surge, sway and yaw direction which are low frequency motion since DP system normally controls low frequency motion.

Table 7 Ice load cases for GEM simulation

Case No.	Ice thickness	Density	Drift speed	Crushing strength	Heading
	[m]	[kg/m^3]	[m/s]	[Mpa]	[deg]
1	1.0	850	0.5	2.0	0~50
2	1.0	900	0.5	1.8	0~50
3	1.0	900	0.5	2.0	0~50
4	1.0	900	0.5	2.2	0~50
5	1.0	900	0.8	2.0	0~50
6	1.0	900	0.9	2.0	0~50
7	1.0	900	1.0	2.0	0~50
8	1.0	950	0.5	2.0	0~50
9	1.5	900	0.5	2.0	0~50
10	2.0	900	0.5	2.0	0~50

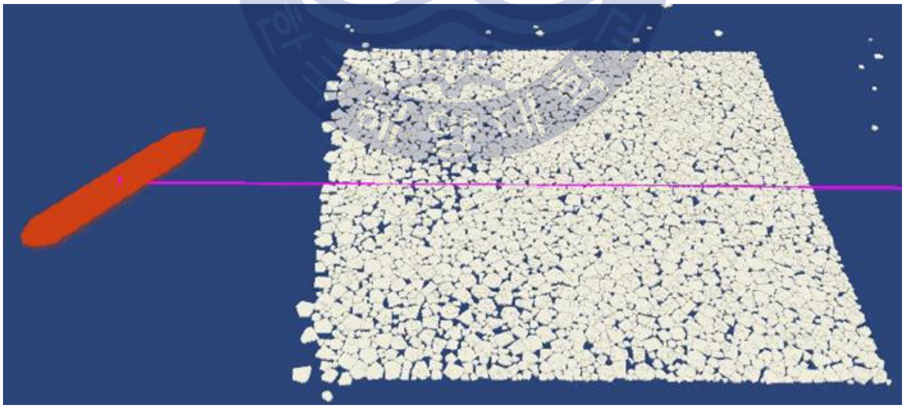

Fig. 17 Rotated vessel heading for ice drift direction (Han et al., 2017)

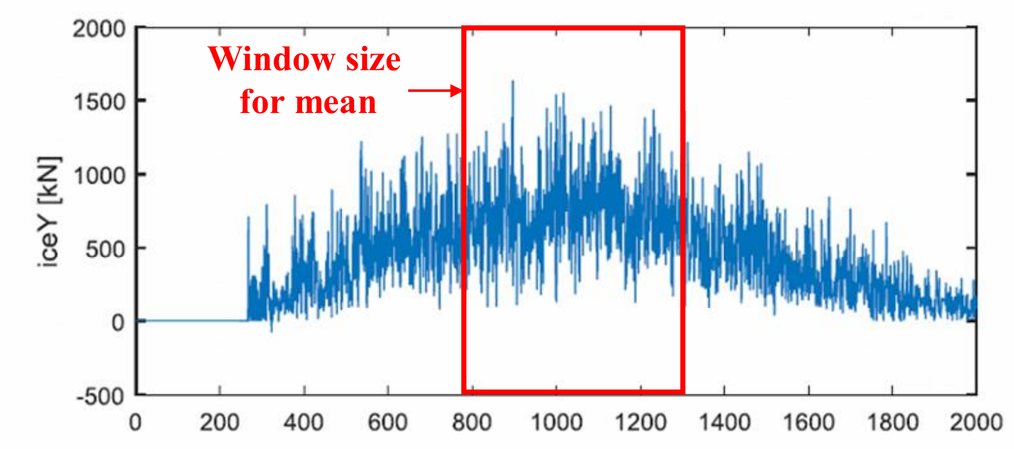

Fig. 18 Ice load example by GEM (Han et al., 2017)

3.3.3 Environmental condition

Wind and current force can be calculated using wind and current coefficient by model test or numerical simulation and projection area of model. In this thesis, wind and current coefficient is based on CFD analysis result of model. Maximum wind speed for generating DP capability plot is 50 m/s and steady wind condition. Normally, DP system does not compensate the high frequency motion because of fuel-efficiency and wear and tear. Therefore, wave drift force by second wave excitation force is used for computation of wave force. According to IMCA, wave condition for calculating wave drift force can be determined by relation with wind speed as shown Table 8. Once wind speed is suggested, wave spectrum containing parameters from Table 8 can be produced. Using wave spectrum and transfer function for mean drift force, wave load can be calculated.

Table 8 Wind-wave relation in IMCA

Sig. Wave Height Hs [m]	Crossing Period Tz [s]	Peak Period Tp [s]	Mean Wind Speed Vw [m/s]
0	0	0	0
1.28	4.14	5.3	2.5
1.78	4.89	6.26	5
2.44	5.72	7.32	7.5
3.21	6.57	8.41	10
4.09	7.41	9.49	12.5
5.07	8.25	10.56	15
6.12	9.07	11.61	17.5
7.26	9.87	12.64	20
8.47	10.67	13.65	22.5
9.75	11.44	14.65	25
11.09	12.21	15.62	27.5
12.5	12.96	16.58	30
13.97	13.7	17.53	32.5
15.49	14.42	18.46	35

3.3.4 Generation of DP capability plot

Using generated environmental force and thruster information, wind and thrust envelop for analysis of DP capability under ice condition is calculated. Depending on Table 7, 10 DP capability plots are produced. Fig. 19, 20, 21, 22 is thrust envelope with respect to variation of ice parameters. Below of every thrust envelope, environmental condition is defined. V_c is current velocity, V_w is wind velocity, $H_s$is significant height. T_z is zero-crossing period.

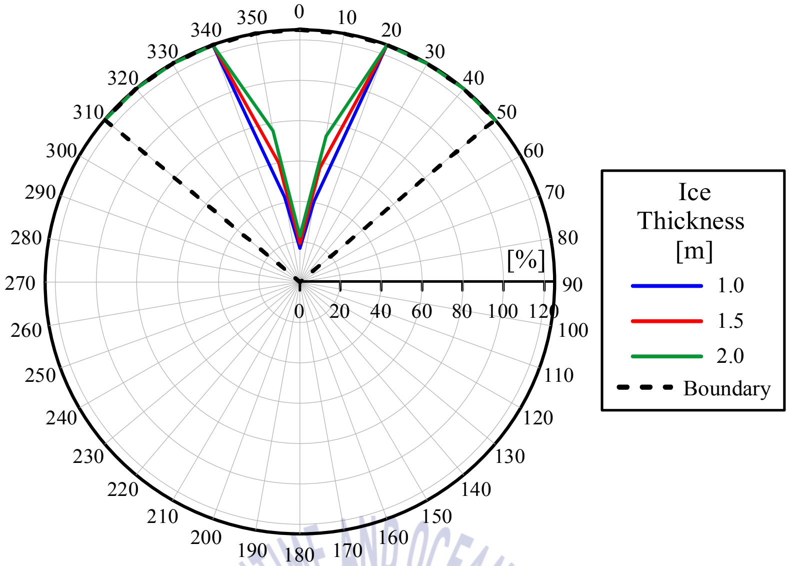

$\mathbf{V_c}$ **: 1 m/s,** $\mathbf{V_w}$ **: 10 m/s,** $\mathbf{H_s}$ **: 3.21 m,** $\mathbf{T_z}$ **: 6.57 s**

Fig. 19 Thrust envelope with respect to ice thickness

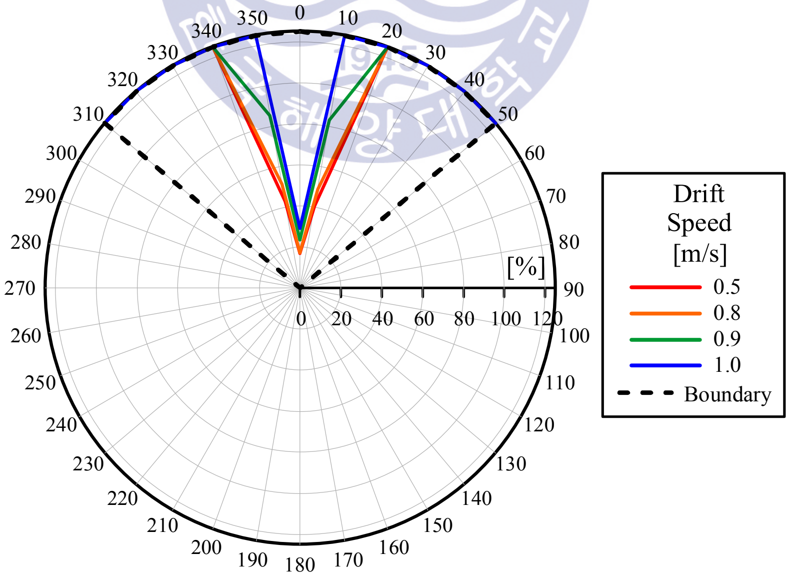

$\mathbf{V_c}$ **: 1 m/s,** $\mathbf{V_w}$ **: 10 m/s,** $\mathbf{H_s}$ **: 3.21 m,** $\mathbf{T_z}$ **: 6.57 s**

Fig. 20 Thrust envelope with respect to ice drift speed

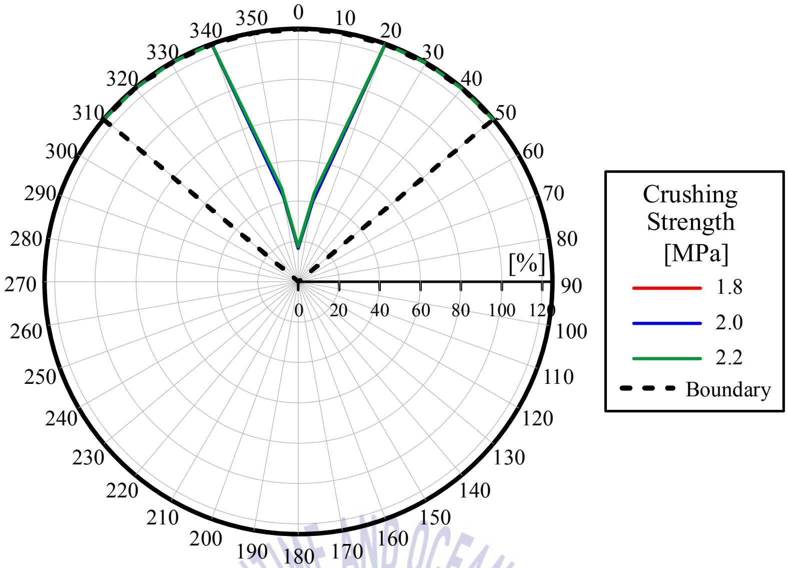

V_c : 1 m/s, V_W : 10 m/s, H_S : 3.21 m, T_z : 6.57 s

Fig. 21 Thrust envelope with respect to crushing strength

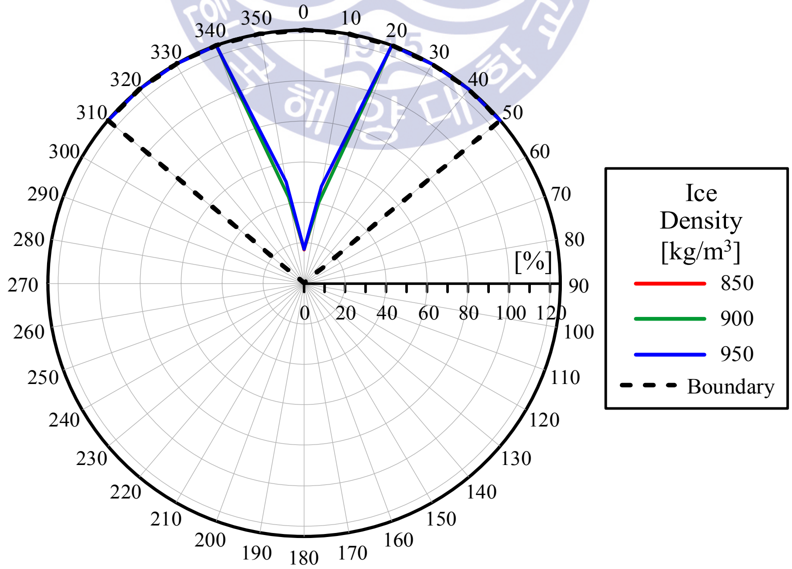

V_c : 1 m/s, V_W : 10 m/s, H_S : 3.21 m, T_z : 6.57 s

Fig. 22 Thrust envelope with respect to ice density

In this result, main objective is to confirm the station keeping range of DP system depending on ice parameter. Therefore, thrust envelopes are used for comparison not wind envelop. Each graph, result is specified up to ±50 degree from heading of vessel using dot line as a boundary. Since when the condition of no ice load is applied at angle of more than ±50, the required thrust exceeds the available thrust, boundary is determined ±50 degree. In thrust envelop, it is good capacity when the result is close to the origin. The effect of ice parameters on DP performance is analyzed by comparing the average sensitivity between ice parameters. Sensitivity represents the ratio of the thrust envelope value variation to the parameter variation at the direction of 10. Sensitivity can be calculated using Eq (16). Sensitivity used for comparison is mean sensitivity which is specified in Table 9. △Thrust envelope is variation of thrust envelope at the direction of 10 and this is named as maximum thrust variation. Since the lower the sensitivity, the less the variation in the maximum thrust depending on the variation of parameter, the influence of the parameter on the thrust is small.

$$Mean\, sensitivity = E\left(\frac{\triangle Thrust\, envelope}{\triangle P}\right) \tag{16}$$

$\triangle Thrust = variation\ of\ thrust\ envelope\ value$

$\triangle P = Variation\ of\ parameter\ value$

Table 9 Result of sensitivity calculation

	ΔP (Variation)	ΔThrust envelope	Sensitivity	Mean sensitivity (E(sensitivity))
Thickness	0.5 (1m →1.5m)	2.58	5.15	5.94
	0.5 (1.5 →2.0m)	3.36	6.72	
Drift speed	0.3 (0.5 →0.8 m/s)	0.27	0.90	40.44
	0.1 (0.8 →0.9 m/s)	6.29	62.9	
	0.1 (0.9 →1.0 m/s)	5.75	57.5	
Crushing strength	0.2 (1.8 →2.0 MPa)	0.54	2.68	2.67
	0.2 (2.0 →2.2 MPa)	0.53	2.65	
Ice density	50 (850 →900kg/m^3)	0.40	0.01	0.01
	50 (900 →950kg/m^3)	0.11	0.01	

3.4 Discussion

In order to check Ice parameters which affect DP capability, result analysis is conducted following Table 10.

Table 10 Result comparison scenario

	Ice thickness	Density	Drift speed	Crushing strength
Case no.	3,9,10	3,5,6,7	2,3,4	1,3,8

Firstly, from the Table 9, Sensitivity in all ice parameters shows variation which means all ice parameters affect DP thrust. However, the differences of sensitivity with respect to ice parameters exist and especially, the crushing strength and density is minute sensitivity value than drift speed. Accordingly, DP capability variation based on crushing strength and density is judged to be insensitive as shown in Fig. 21 and 22. In particular, since the sensitivity of ice density is very small, it is judged that it will not have a significant impact on DP performance even if simulated by fixing it to the ice density of 920kg/m^3, which is commonly used in DP simulations under ice conditions.

Secondly, according to the mean sensitivity of Table 9, the ice thickness is

8 times smaller than the drift speed, and the thruster saturation angle is fixed with 20 degree with respect to the parameter variation, so the DP performance is not sensitive. Nevertheless, noticeable change due to the thickness variation shown in Fig. 19 is observed. Therefore, the ice thickness can be one of the important parameters of the DP simulation and should be simulated based on the ice thickness data of the target field.

Thirdly, According to Table 9, the result of the ice drift speed shows that the sensitivity difference and mean sensitivity is quite large. When the parameter variation of drift speed is 0.3, the sensitivity is 0.9 and also when parameter variation is 0.1, the sensitivity is 62.9 and 57.5. This result shows that considerable nonlinear tendency depending on the parameter variation. At this point it is necessary to evaluate the rationality of statistical processing used in calculating the ice load. Because the ice load is extremely fluctuated environmental condition with respect to time, the ice can respond to impulses according to conditions, and it can also be in a non-continuous form. For that reason, since irrational values can be produced in the process of calculating the mean value, the drift speed used in the analysis is 0.8, 0.9, and 1.0 m/s, excluding nonlinear intervals. From the result of range 0.8~1.0 m/s, drift speed shows the most sensitive tendency. Also, the change of saturation angle is observed in Fig. 20.

Therefore, it is a parameter that has the greatest impact on DP performance reduction. This may related to the assumption that the ice drift speed is consistent with the current velocity, which means that the analysis of the current velocity in the target sea area should be done in detail. As a result, in simulation considering drift speed, various drift speeds should be considered by setting a finer interval than the parameter variation used in this simulation.

As a conclusion, the following five conclusions are drawn :

(1) When the value of all the ice parameters increase, the DP performance decrease.

(2) The drifting speed of the ice is very sensitive to DP performance and has the greatest impact.

(3) The ice thickness is one of the parameters that must be considered in simulation.

(4) The ice crushing strength and density do not have a significant impact on DP performance.

(5) Statistical properties that can consider fluctuation of ice load are required when calculating ice load from time history.

From the result, DP simulations with ice conditions should be considered as a priority for ice thickness and drift speed, and ice crushing strength and density can be used for fixed values in DP simulation or excluded from major parameters for DP performance analysis.

Chapter 4. Heading control

4.1 Overview

This chapter introduces new heading control method for DP assisted mooring system under ice condition using tension in real-time.

It is obvious that the stable heading control is to align the heading with ice drift direction. To establish this condition, it is crucial to determine the direction of ice drift. Normally, At the real operation, It is possible to do feed-forward control since DPO controls heading and position with information of ice drift direction from buoys, sensors or visualized ice concentration information(Kerkeni & Metrikin, 2013). However, the automatic controls can be a reactive method with only estimated information of platform such as tension, position and velocity. In the reactive method, it can be difficult to determine ice drift direction. Tension can be increased or decreased by ice under ice condition since ice is dominant environmental load than other loads which are wave, current and wind(Kerkeni et al., 2013). Therefore, Ice drift direction can be estimated through the tendency of tension rising as shown Fig. 23. In order to match the target heading and ice drift direction, the strategy for target heading can be set following the most loaded line.

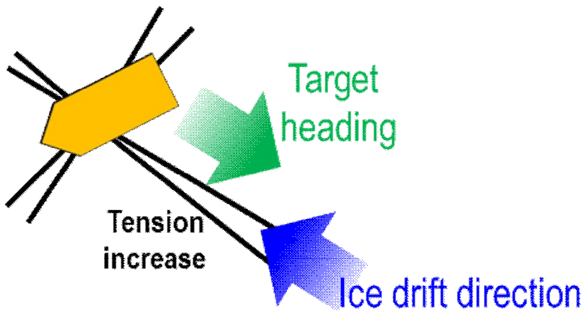

Fig. 23 Strategy for target heading

4.2 Strategy for heading control

The heading control in this thesis is focusing on the ice load direction dominantly. Depending on the concept for ice detection, target heading is determined using the most loaded and second loaded lines in this study. It can be dangerous to detect ice drift direction using only one line. Therefore, the ratio of two lines are compared to determine target heading. The target heading is specified by adding a weight to the side where the tension is higher among the two lines.

T_1 specified at Eq (17) is the most loaded line and T_2 is second loaded line. R is a weight of T_1 between T_1 and T_2. By multiplying R to difference of angle which is Eq (18) between line T_1 and T_2, ratio of angle for T_1 is calculated. Finally, according to Eq (19), target heading is determined summing angle ratio for T_1 and $Angle_{T_2}$. Target heading is always determined closely to the most loaded line as shown Fig. 24 following Eq (17)~(19).

$$R = \frac{T_1}{T_1 + T_2} \tag{17}$$

$T_1 = The\ most\ loaded\ line$

$T_2 = Second\ loaded\ line$

$$Gap_{angle} = Angle_{T_1} - Angle_{T_2} \tag{18}$$

$$Target\ Heading = Angle_{T_2} + Gap_{angle} \times R \tag{19}$$

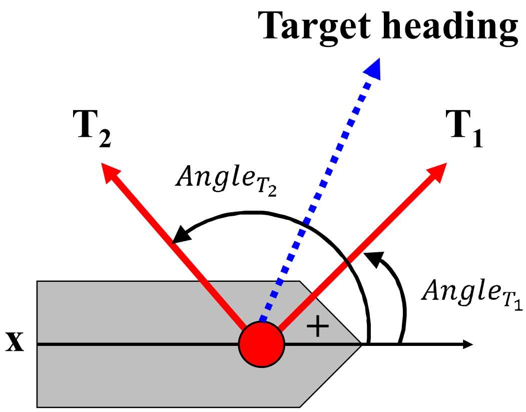

Fig. 24 Calculation of target heading

In the process of calculating target heading, the determination of the most loaded and second loaded lines are crucial process. This process is processed by Fig. 25. The tension for target heading is determined by mean of each line’s tension with certain window size as show Fig. 25. If the window size is too small, the variation of calculated target heading will be too severe. On the other hands, the reasonable tension can not be included in calculation of target heading when the window size is too big. Therefore, window size is required to be determined with the characteristic of tension response for each system. According to the window size, mean tension during window size for each line can be calculated by following Fig. 25. Then the most loaded line which is T_1 and the second loaded line which is T_2 are determined to calculate target heading.

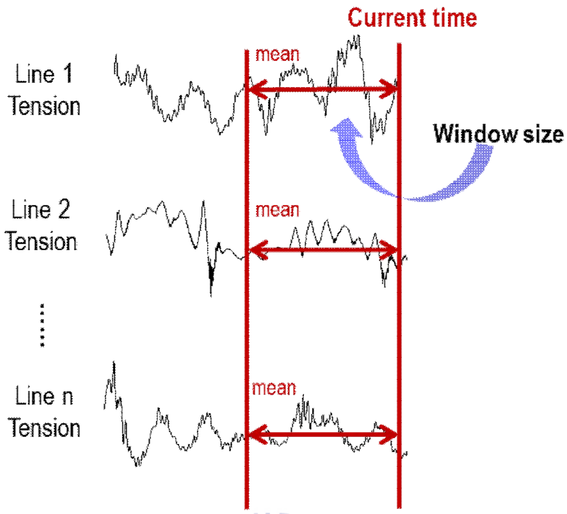

Fig. 25 The concept of window size

Using the calculated tension, target heading is calculated using the most loaded line and second loaded line depending on Eq (17)~(19).

4.3 Simulation with heading control

In order to validate the performance of suggested heading control strategy, case studies are conducted. During 2 hours simulation, the heading control of DP system is conducted in the ice drifting condition from various directions,

4.3.1 Cases

The 4 simulation cases of heading control(HC) with suggested strategy and with no heading control(NHC) are compared to check heading keeping ability. Ice drift directions of each cases are different each other. Details of 4 cases for simulation is summarized in Table 11.

Table 11 Simulation case about heading control

Case no.	Initial Heading [deg.]	Ice drift direction [deg.]	Simulation time [s]	Case configuration
1	0	+45	7200	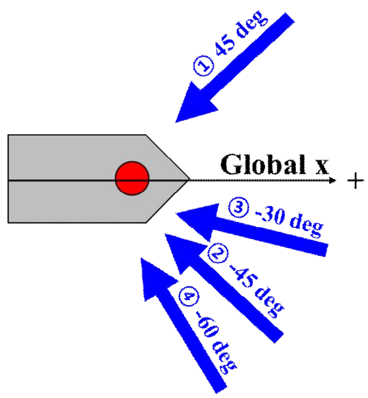
2	0	-45	7200	
3	0	-30	7200	
4	0	-60	7200	

4.3.2 Ice loads

The platform, mooring and DP system for simulation are specified at paragraph of 2.2.4. Case studies are performed with only ice load since dominant characteristic of ice compared to other environmental loads in case of the DP assisted mooring system. The ice load is assumed using impulse function as shown Fig. 26. The assumption of impulse function is close to big impact between platform and ice like pack ice. The production operation in Arctic Ocean is almost possible with management of ice with ice breaker. Therefore, the ice should be assumed as managed ice which is close to a continuous function. However, this study is conducted with ice of simple impulse function to evaluate feasibility of control strategy. Ice load specified in Fig. 26 is loaded to the center of platform in simulation.

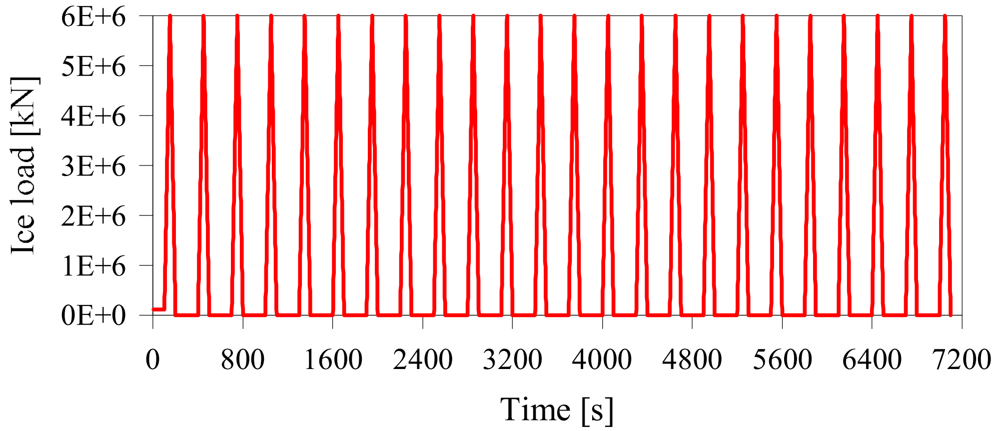

Fig. 26 Simulated ice load as impulse function

4.3.3 Procedure for heading control

Following the simulation case of Table 11, the simulation is processed by the procedure of Fig. 27. For each window size, the most and second loaded lines are calculated. Also, the target heading using both lines is calculated. In this stage, the calculated target heading is judged by two boundary conditions in Fig. 27. The first boundary condition is the difference between current and target heading. The heading control is only performed when the difference between target heading and current heading exceeds 5 degree. From the result of Fig. 19, 20, 21 and 22, thruster is saturated when the ice is coming to platform with the direction of 10 degree. It notes that the relative angle with ice should be within 10 degree for stable DP operation. Considering this notation, the limitation for control of heading is determined as 5 degree in this study. If calculated heading is not over the 5 degree, the heading controller detects tension again. The second boundary condition is tension difference. The target heading is calculated by focusing on the line's tension. During the ice load is acting on the platform, the heading control may not be necessary when the tension difference of all lines are small. It is judged that the platform is not so dangerous when the tension difference is too small. Therefore, in order to prevent excessive fuel consumption, the heading control is conducted when the most and lowest loaded line's tension is over the 2000kN as shown Fig. 27. If the two boundary conditions are satisfied, DP starts the control to the target heading.

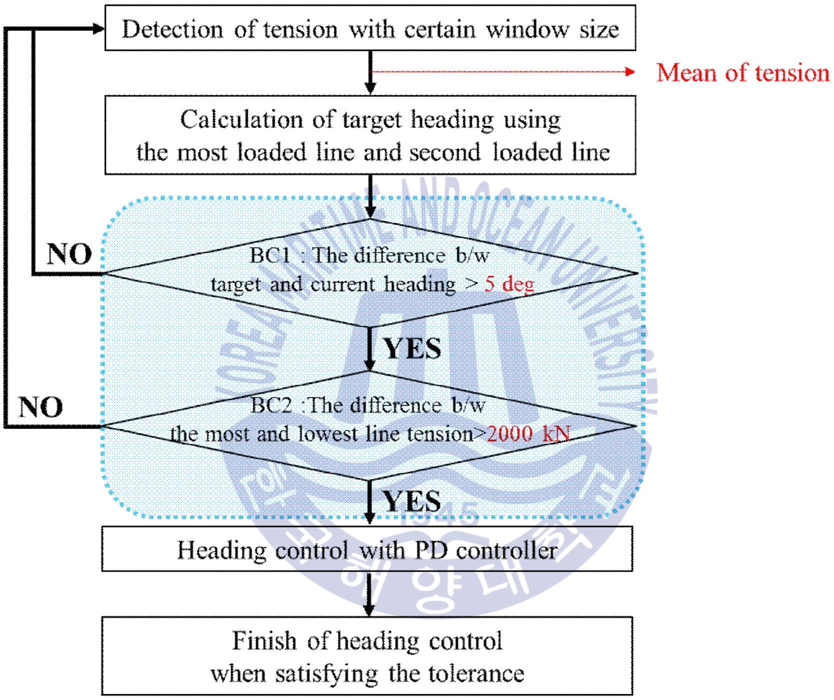

Fig. 27 Simulation process for heading control

4.4 Result of heading control

4.4.1 Case 1

Fig. 28 shows the 2 hours simulation with heading control when the ice load is acting along the 45 degree from the platform's heading direction. In this case, the ice drift direction is located within mooring line bundles #1. As shown in Fig. 28(a), the target heading is set around 45 degree at which the ice drift is coming from. It is shown that the control to target heading shows good agreement with ice drift direction compared with the cases of no heading control. And in the result of Fig. 28(b), the red line with heading control is closer to 45 degree than the black line without heading control. The advanced performance is found when the ice load acts on the bundle of mooring system accurately.

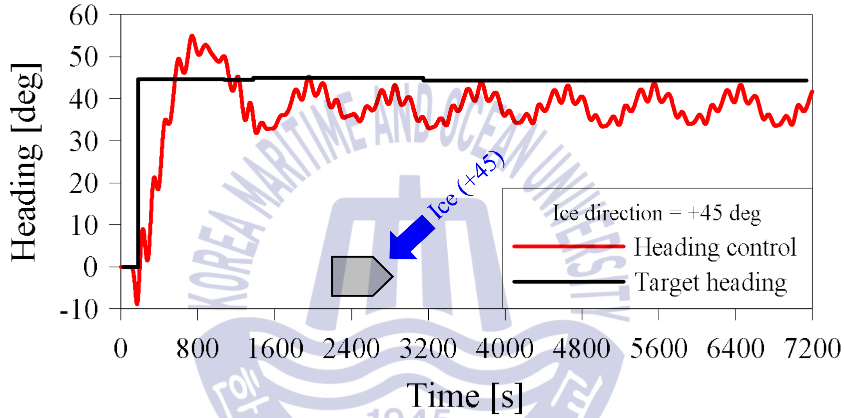

(a)

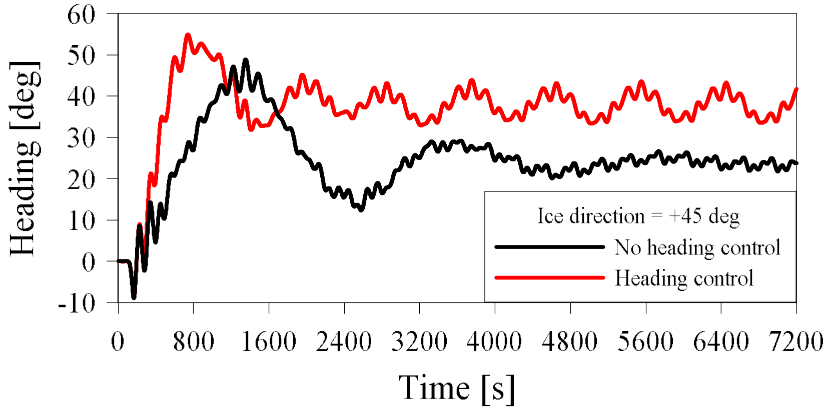

(b)

Fig. 28 Heading time history of case 1

4.4.2 Case 2

In case 2, ice is drifted from −45 degree that is in the middle of mooring line bundle #4. The good agreement of calculated target heading with the ice drift direction which is −45 degree is shown in Fig. 29(a) as case 1. Also, from the result of Fig. 29(b), the heading control compared with no heading control shows advanced detection close to ice drift direction.

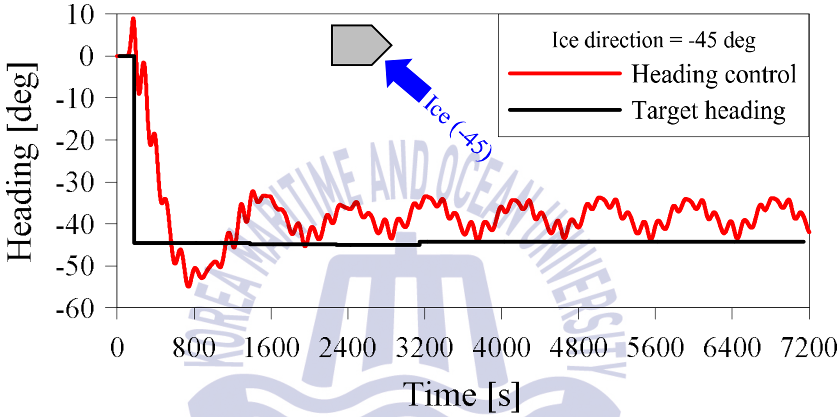

(a)

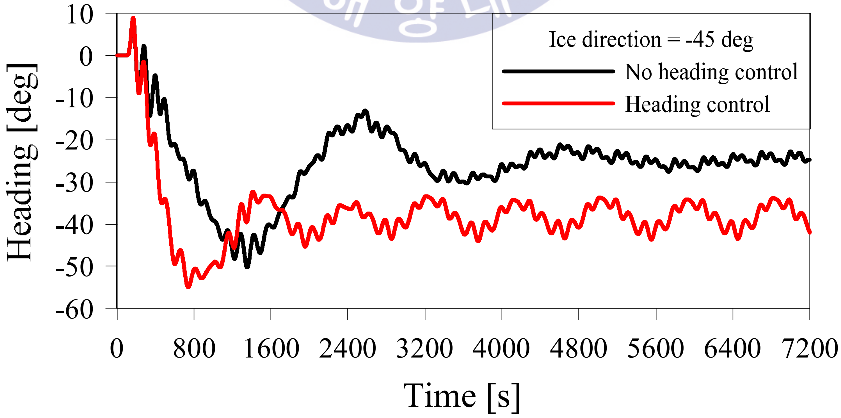

(b)

Fig. 29 Heading time history of case 2

4.4.3 Case 3

The case 3 is a result when the ice is drifted from -30 degree that is not located inside of any mooring line bundle. From the result of Fig. 30(a), the target heading is calculated close to -44 degree. The calculated target heading shows difference from ice drift direction. It is because that the strategy to calculate target heading is using most and second loaded mooring lines. In Fig. 31, the closest line to the ice direction of -30 degree is the line #16 with -44 degree. This configuration of mooring lines and ice direction limits the target heading at -44 degree which is a boundary of mooring line bundle. As a result, It can be said that this strategy determines a good directionality close to ice direction when it is located outside of mooring bundles. Fig. 30(b) represents the good performance of heading control with target heading compared with the case of no heading control.

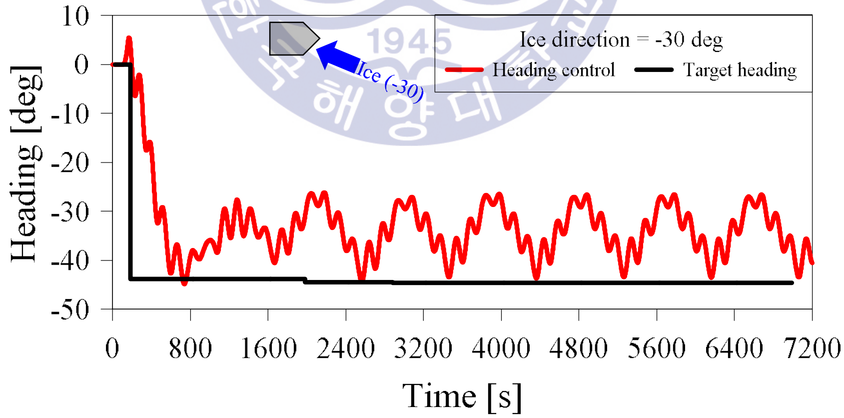

(a)

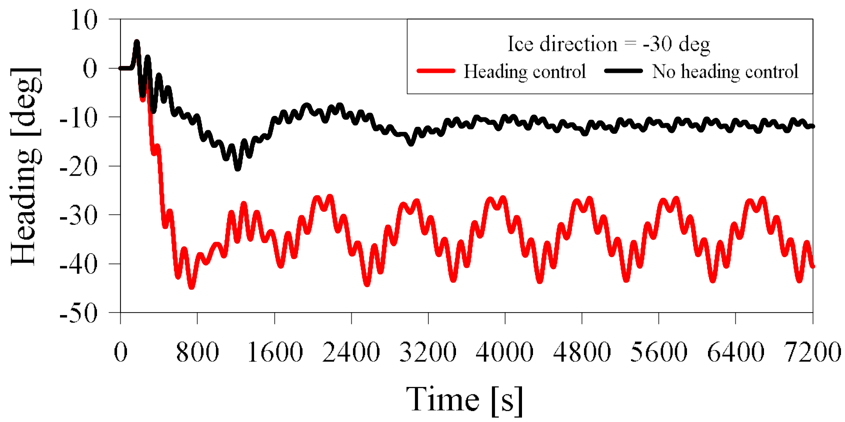

(b)

Fig. 30 Heading time history of case 3

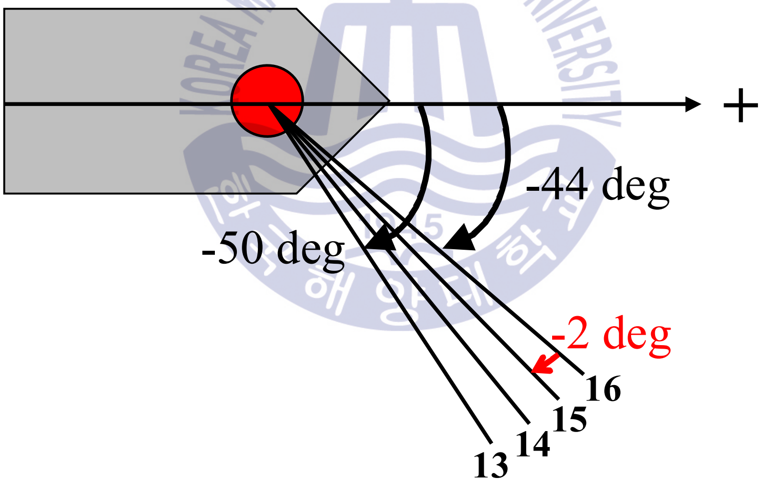

Fig. 31 Angle of bundle 4

4.4.4 Case 4

The ice drift direction of case 4 is −60 degree. In the Fig. 32(a), the target heading is almost −50 degree. This direction has differences from the ice drift direction. Similar with case 3, the ice is acting outside of boundary of mooring line bundle. Therefore, following the strategy, the target heading can be determined as close to line #13 which is the most loaded line under given ice drift direction. In the Fig. 32(b), the tendency of heading with control and without control is not showing remarkable differences. It is because the DP moment due to heading control is coincide with the weather vaning moment on the ship. Nevertheless, the strategy for target heading finds proper directionality for heading control to ice drift direction.

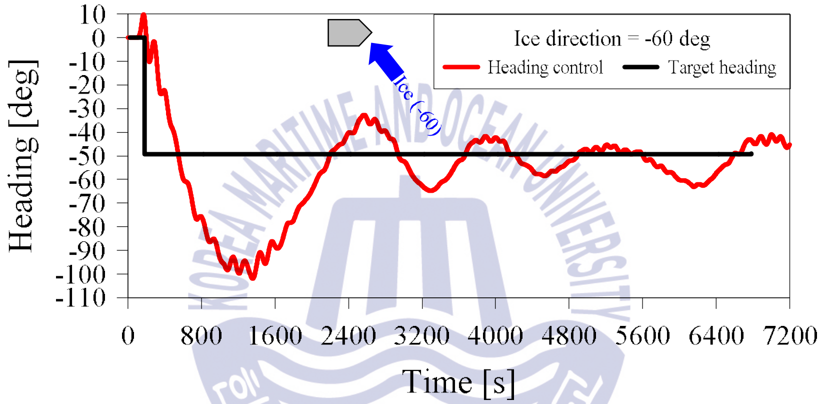

(a)

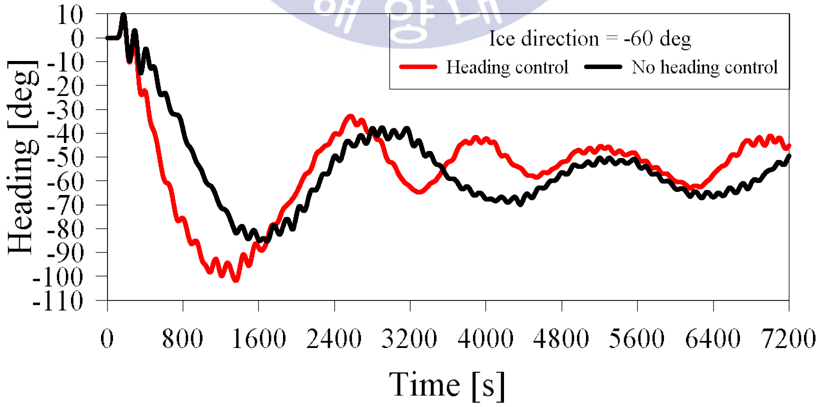

(b)

Fig. 32 Heading time history of case 4

Chapter 5. Conclusion

This thesis suggests a new strategy of station-keeping for DP assisted mooring system in Arctic ocean. The strategy is consisted of position control for surge, sway and heading control. New position control determines SP for surge and sway using tension estimation method. The tension for SP is determined by two components: the local tension and global tension. The local tension estimation reflects tension variation during certain time window and gives a directionality. The global tension which is the result of static analysis represents the tendency of tension with respect to the change of offset of the vessel. At the area of superposed both components, a position where has minimum tension calculated from both local tension and global tension is determined as the SP. This strategy is to be proven to generate reasonable SP with the purpose of the reduction of tension.

For control strategy under ice condition, the most influential ice parameter and the ice characteristic which affects control of platform are analyzed by static analysis of DP system. The DP capability plots representing the capability of DP system with various ice parameters are generated. From the result, it is shown that ice thickness and drift velocity are important ice parameters for determination of DP capability. Also, aligning vessel heading direction and ice drift direction within certain limit considering DP performance can be crucial to improve heading control quality.

Based on the result of static analysis considering ice parameters, new heading control strategy is suggested using time history of tension in real-time. The strategy for the calculation of target heading using both the most and second loaded line. Case study to validate the suggested heading control strategy are performed. From the simulation with 4 different ice drift directions, the advanced performance in station-keeping of heading compared with the cases of no heading control is validated. When ice load direction is located inside of mooring bundle, the intuitive determination of ice load direction is observed. When ice load direction is outside of mooring bundle, the determination of directionality close to ice drift direction is reasonably predicted. However, this study suggests that the improvement on determination of the target heading is required for better station-keeping capability without fluctuation.

Consequently, the suggested control strategy for DP assisted mooring system will enable both safe operation with fuel-efficiency and improved operation of ice breakers.

Reference

최진우, 김세원, 류민철, & 김용수., 2012. Azimuth Thruster 설계변수에 따른 Dynamic Positioning Capability 의 영향 분석. *대한조선학회 학술대회자료집,* 858-863.

Barth Berntsen, P.I., Aamo, O.M. & Leira, B.J., 2008. *Thruster assisted position mooring based on structural reliability,* International Journal of Control, 81(9), pp 1408-1416.

Daley, C., Alawneh, S., Peters, D., Quinton, B. & Colbourne, B., 2012. *GPU modeling of ship operations in pack ice.* International Conference and Exhibition on Performance of Ships and Structures in Ice, September, Banff Alberta, Canada, pp. 20-23.

Daley, C., Alawneh, S., Peters, D. & Colbourne, B., 2014. *GPU-event-mechanics evaluation of ice impact load statistics.* OTC Arctic Technology Conference, Offshore Technology Conference

Han, S.L., Kim, H.J., Lee, D.Y. & Kim, B.K., 2017. Capability Analysis of Dynamic Positioning for the Arctic FPSO in ICE. *Proceeding of the 24th International Conference on Port and Ocean Engineering under Arctic Conditions,* June 11-16, Busan, Korea.

International Marine Contractors Association(IMCA)., 2000. *Specification for DP capability plots.* IMCA M140.

International Towing Tank Conference(ITTC)., 1999. *Testing and Extrapolation Methods Ice Testing General Guidelines.* ITTC Recommended Procedures and Guidelines, No. 7.5-02-04-01.

Jenssen, N. A., Hals, T., Jochmann, P., Haase, A., Dal Santo, X., Kerkeni, S., Kerkeni & Metrikin, I., 2012. *DYPIC – A Multi-National R&D Project on DP Technology in Ice.* Dynamic Positioning Conference, Marine Technology Society, Houston, Texas.

Jung, K.H., Lee, M.K.. & Shin, S.Y., 2017. Design Considerations and Analysis of Arctic FPSO's Turret Moorisng System. *The Autumn Conference of The Korea Society of Ocean Engineers,* Geojedo, Korea.

Kongsberg Maritime AS, 2015. *DP Capability Analysis K-Pos DP-21 and cJoy Relume,* Kongsberg Maritime AS

Liferov, P., McKeever, T., Scibilia, F., Teigen, S. H., Kjøl, A., Almkvist, E., Lindvall, J. K. 2018. STATION-KEEPING TRIALS IN ICE: PROJECT OVERVIEW. Proceedings of the ASME 2018 37th International Conference on Ocean, Offshore and Arctic Engineering(OMAE) June 17-22, 2018, Madrid, Spain

Nguyen, D. T. & Sørensen, A. J., 2009. *Setpoint chasing for thruster-assisted position mooring.* IEEE Journal of Oceanic Engineering, 34(4), 548-558.

Nguyen, D. T., Sørbø, A. H. & Sørensen, A. J., 2009. *Modelling and control for dynamic positioned vessels in level ice.* IFAC Proceedings Volumes, 42(18), 229-236.

RMRS., 2016, *Rules for the Classification and Construction of Sea-Going Ships, Part I - CLASSIFICATION.* Russia Maritime Register of Shipping, Russia.

Ryu, S. & Kim, M. H., 2003. Coupled dynamic analysis of thruster-assisted turret-moored FPSO. *In OCEANS 2003 Proceedings* Vol(3), pp. 1613-1620. IEEE.

Strand, J. P., Sørensen, A. J. & Fossen, T. I., 1998. *Design of automatic thruster assisted mooring systems for ships.* pp. 61-75.

Strand, J.P., 1999. *Nonlinear Position Control Systems Design for Marine Vessels,* Norwegian University of Science and Technology, PhD thesis, Norway, Trondheim.